

Geology of the Mitchell Au-Cu-Ag-Mo porphyry deposit, northwestern British Columbia, Canada

Gayle E. Febbo^{1, a}, Lori A. Kennedy², Michael Savell³, Robert A. Creaser⁴, and Richard M. Friedman⁵

¹ Mineral Deposit Research Unit, University of British Columbia, Vancouver, BC, V6T 1Z4

² Department of Earth, Ocean and Atmospheric Science, 2020-2207 Main Mall, University of British Columbia, Vancouver, BC, V6T 1Z4

³ Seabridge Gold Inc., 106 Front Street East, Suite 400, Toronto, ON, M5A 1E1

⁴ The 1-26 Earth Sciences Building, University of Alberta, Edmonton, AB, T6G 2R3

⁵ Pacific Centre for Isotopic and Geochemical Research, University of British Columbia, Vancouver, BC, V6T 1Z4

^a corresponding author: Gayle.Febbo@gmail.com

Recommended citation: Febbo, G.E., Kennedy, L.A., Savell, M., Creaser, R.A., and Friedman, R.M., 2015. Geology of the Mitchell Au-Cu-Ag-Mo porphyry deposit, northwestern British Columbia, Canada. In: Geological Fieldwork 2014, British Columbia Ministry of Energy and Mines, British Columbia Geological Survey Paper 2015-1, pp. 59-86.

Abstract

The Mitchell Au-Cu-Ag-Mo porphyry deposit, hosted by Early Jurassic volcanosedimentary and intrusive rocks in the Stikine terrane of northwestern British Columbia, is considered the largest undeveloped gold resource in Canada. It contains 1740 Mt of measured and indicated resource grading 0.61 g/t Au, 0.17% Cu, 3.1 g/t Ag, and 58 ppm Mo based on a 0.5 gold-equivalent gram per tonne cut-off. The deposit is genetically related to multiple diorite intrusions (Sulphurets suite) that cut sedimentary and volcanic rocks of the Stuhini Group (Upper Triassic) and sandstones, conglomerates, and andesitic rocks of the Jack Formation (basal Hazelton Group; Lower Jurassic). Mineralization and accompanying alteration and stockwork proceeded in four stages. Hosted by Phase 1 plutons (196.0 ± 2.9 Ma and 189 ± 2.8 Ma), Stage 1 sheeted veins and stockwork contain most of the copper-gold mineralization and potassic and propylitic alteration. A Stage 2 disseminated and stockwork-hosted molybdenum halo (190.3 ± 0.8 Ma; Re-Os) is peripheral and contiguous with the core copper-gold system. It is associated with phyllic alteration and is temporally related to a Phase 2 pluton (192.2 ± 2.8 Ma) that outcrops central to the halo. Stage 3 consists of poorly mineralized massive pyrite veins associated with advanced argillic alteration and is related to Phase 3 diorite, diatreme breccia emplacement and intrusion breccia dikes. Stage 4 consists of high-level, gold-rich veins that are lateral to, and overprint, the main deposit. The geochemistry of the Sulphurets intrusions, nature and extent of alteration assemblages, high silica content of the ore zone and Mo mineralization, indicate that the Mitchell porphyry is calc-alkalic rather than alkalic. The subalkaline Sulphurets suite is here interpreted as the progenitor to the Mitchell deposit, rather than the alkaline Premier suite. The Premier and Sulphurets suites accompanied siliciclastic sedimentation and andesitic volcanism recorded by the Jack Formation. The deposit was deformed during development of the Skeena fold and thrust belt (mid-Cretaceous) and is now exposed in an erosional window beneath the Mitchell thrust fault, which separates it from its interpreted offset (Snowfield deposit) in the hanging wall to the southeast.

Keywords: Mitchell, Snowfield, Cu-Au porphyry, Kerr-Sulphurets-Mitchell, KSM, Sulphurets district, Iskut, Triassic-Jurassic porphyry, Jack Formation

1. Introduction

The Mitchell Cu-Au-Ag-Mo porphyry deposit is in the Stikine terrane of northwestern British Columbia (Fig. 1). Together, the Kerr-Sulphurets-Mitchell porphyry deposits (KSM), the Brucejack high-grade gold deposit, and the Snowfield porphyry deposit are hosted in volcanosedimentary rocks of the Stuhini Group (Triassic) and unconformably overlying volcanosedimentary strata and allied plutonic rocks of the Hazelton Group (Lower Jurassic; Fig. 2). Part of the Sulphurets district, these deposits lie at the northern end of a 60 km long north-northwest trending Cu-Au porphyry and related mineralization trend that extends south to the town Stewart (Fig. 2). The origin of the trend has been ascribed to Jurassic faults that controlled sedimentation of the Jack

Formation (basal Hazelton Group; Henderson et al., 1992; Lewis, 2001; Nelson and Kyba, 2014), which partly hosts mineralization at KSM, Snowfield and Brucejack.

The Mitchell deposit, delineated by extensive drilling that began in 2006, is considered the largest undeveloped gold resource in Canada (Visual Capitalist, 2013). Although porphyry-related mineralization in the Mitchell zone has been studied for over 50 years (e.g., Kirkham, 1963; Margolis, 1993; Aldrick and Britton, 1991; Lewis, 1992), detailed deposit-scale documentation has hitherto been lacking. Herein we present new field, petrographic, geochemical, and geochronologic data to document relationships between sedimentation, plutonism, alteration, vein paragenesis, mineralization, and deformation.

2. Geologic setting

The Quesnel and Stikine arc terranes are part of the Intermontane Belt of the Canadian Cordillera, geographically

Errata to the printed version of this paper were corrected January, 2019.

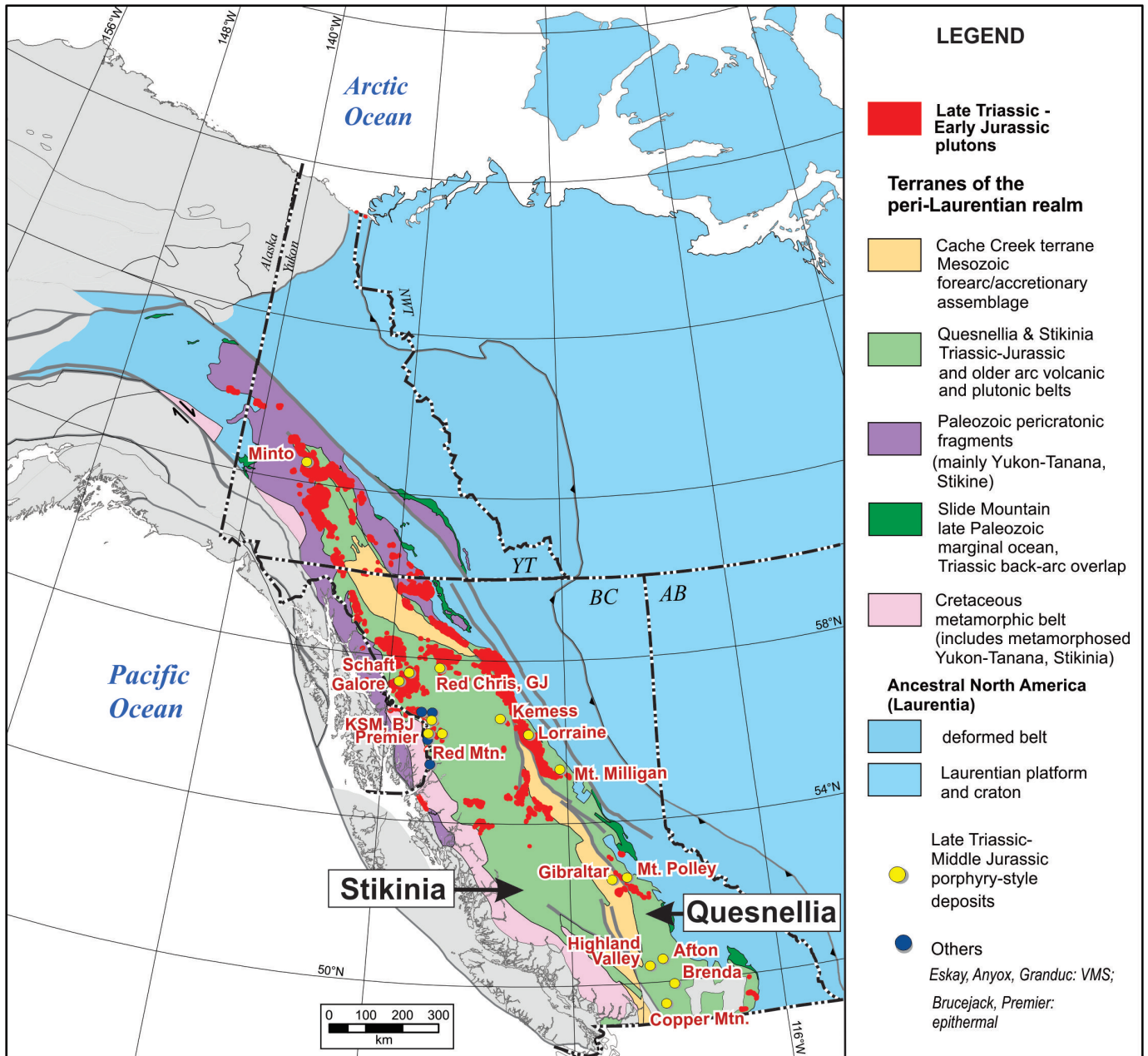


Fig. 1. Tectonic setting of Kerr-Sulphurets-Mitchell (KSM) deposits and other Triassic-Jurassic porphyry and related deposits in Quesnellia and Stikinia (from Nelson and Kyba, 2014).

inboard of the Cost Plutonic Complex and separated from each other by primitive arc and oceanic rocks of the Cache Creek terrane (Fig. 1). Long-lived arc magmatism across Stikinia and Quesnellia during the Late Triassic to Early Jurassic generated paired belts of alkalic and calc-alkalic porphyry deposits that extend for 2,000 km along the axis of the Canadian Cordillera (Logan and Mihalynuk, 2014). These deposits are both alkalic (e.g., Afton-Ajax, Copper Mountain, Mount Polly and Galore Creek) and calc-alkalic (e.g., Gibraltar, Schaft Creek and Kemess). Porphyry deposits of the Sulphurets district are along the western margin of the Stikine terrane (Fig. 1) with mineralization ages between 197 and 190 Ma (Bridge,

1993; Margolis, 1993; this study). Gold mineralization in the Sulphurets district spans ~12 Ma as indicated by high-grade gold-silver at Brucejack (ca. 185 Ma) superimposed onto older porphyry mineralization (192-190 Ma; Pretium Resources, 2013).

The Stikine terrane comprises three unconformity-bounded island arc volcanosedimentary successions that span 200 Ma. These include the Stikine assemblage (Devonian to Mississippian; Anderson, 1989; Greig, 1992; Logan et al., 2000), the Stuhini and Takla groups (Middle to Late Triassic), and the Hazelton Group (Late Triassic to Middle Jurassic). Mesozoic plutonic suites (Figs. 1, 2) include Stikine and

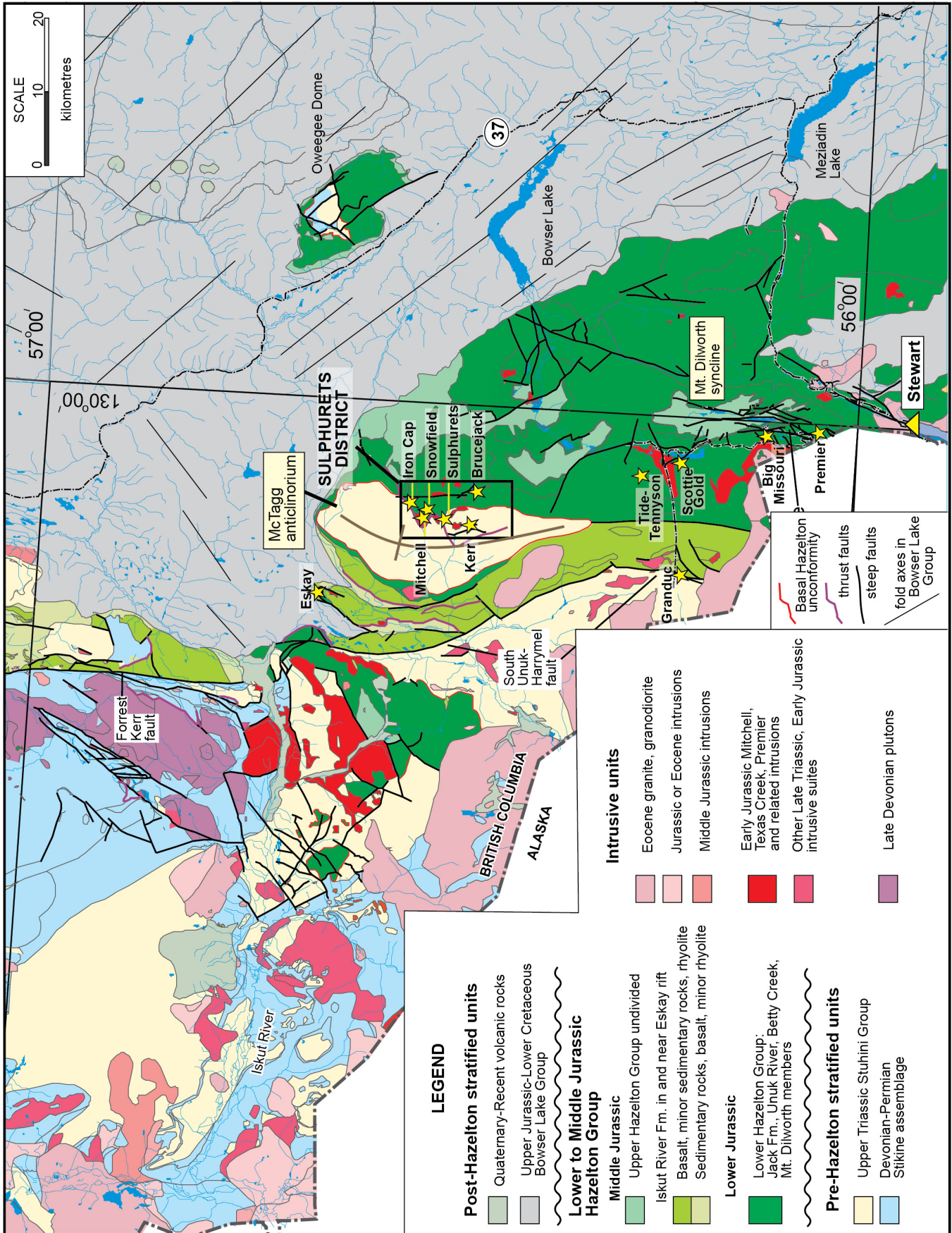


Fig. 2. Western Iskut region geology. The Stewart-Sulphurets district trend extends from the Premier deposit ~ 60 km north to the Sulphurets district (from Nelson and Kyba, 2014).

Copper Mountain (Late Triassic, coeval and comagmatic with the Stuhni Group), Texas Creek (coeval and comagmatic with the Hazelton Group; Early Jurassic), Three Sisters (Middle Jurassic). Gold-rich deposits are associated with both the Late Triassic and Early Jurassic intrusive suites in northwestern Stikinia. Between Stewart and the Sulphurets district (Fig. 2) these deposits coincide with a belt of 195-187 Ma Texas Creek plutons (Alldrick, 1993; Logan and Mihalynuk, 2014). The Premier intrusions are an important subset of the Texas Creek plutons named for the synmineral dike occurrences in the Premier mine area near Stewart (Alldrick, 1993). Premier suite rocks are defined in the Stewart area by the presence of potassium feldspar megacrysts and plagioclase phenocrysts ('two-feldspar porphyry') in a fine-grained groundmass (Alldrick, 1993). East of the Sulphurets district, the Bowser Lake Group is a molassoid sedimentary succession containing debris derived from the collision of the Intermontane terranes and the edge of ancestral North America (Evenchick et al., 2007). The area was deformed by mid-Cretaceous sinistral transpression that gave rise to the Skeena fold and thrust belt, an extensive NE-verging zone of shortening that extends across most of the northern Intermontane Belt (Evenchick, 2001). The Sulphurets district is on the eastern limb of the McTagg anticlinorium, a north-trending mid-Cretaceous structural culmination (Fig. 2). The anticlinorium is bounded in part by outward-vergent thrust faults, including the east-vergent Sulphurets fault, structurally above the Mitchell deposit (Figs. 2, 3).

3. Sulphurets district geology

3.1. Stratigraphy

The Sulphurets district is underlain predominantly by Stuhini Group bedded sedimentary rocks and Hazelton Group siliciclastic rocks that interfinger with massive and fragmental andesites, and related Mitchell plutons (Lewis, 2013; Figs. 3-5). Drill holes in the western Sulphurets district intersected maroon radiolarian chert from surface to depths of 200 m that are interpreted to be Stikine assemblage (Nelson, pers. comm., 2014). The chert is located in the bottom of the valley in the hinge area of the McTagg anticlinorium and represents the lowest stratigraphic level identified in the McTagg.

Stuhini Group rocks comprise thinly bedded mudstone, graphitic mudstone, and lesser calcareous mudstone, and felsic tuff. The uppermost Stuhini Group unit immediately beneath the sub-Hazelton Group unconformity consist of felsic volcanic stratified tuffs, fragmental and coherent rocks (Fig. 5).

The base of the Hazelton Group is an angular unconformity that cuts into previously folded Stuhini Group rocks, marking a significant regional hiatus in volcanism and an episode of uplift and erosion (e.g., Nelson and Kyba, 2014). The unconformity is overlain by polymictic conglomerates with felsic intrusive and extrusive clasts and quartz-rich arkoses of the Jack Formation, a unique basal Hazelton unit that is restricted to the periphery of the McTagg anticlinorium (Nelson and Kyba, 2014). In the KSM area, the conglomerate commonly contains black mudstone intraclasts, clasts of black chert, felsic

and intermediate volcanic rock, crowded feldspar porphyry intrusive rock and bedded mudstone. In the Sulphurets district, Jack Formation strata interfinger with, and pass gradationally to, andesitic breccias, flows, and tuffs (Nelson and Kyba, 2014).

Subaerial andesite and dacite volcanic and volcanoclastic strata overlie the Jack Formation in the Brucejack area. They were included in the Betty Creek Formation by Lewis (2013). A thin unit of Middle Jurassic fossiliferous mudstone, also assigned to the Betty Creek Formation, outcrops east of the Iron Cap deposit.

3.2. Plutonism

Small Early Jurassic porphyritic diorite to syenite bodies referred to as the Mitchell intrusions cut the Stuhini and Hazelton groups in the Sulphurets district, and are considered part of the Texas Creek plutonic suite (Kirkham, 1963; Alldrick and Britton, 1988, 1991). We recognize two suites modified from Alldrick and Britton's (1991) 'one-feldspar' Sulphurets Glacier porphyry and 'two-feldspar' Premier porphyry identified in the Sulphurets district (see also Alldrick, 1993). Crowded, coarse-grained Premier intrusions are cut by uncrowded, relatively fine-grained Sulphurets intrusions. The Premier suite, consisting of diorite, monzonite, granite, syenite and quartz syenite, are crowded porphyry intrusions that are commonly medium to coarse grained and contain minor porphyry mineralization. West of the Sulphurets zone and above the Sulphurets thrust, diorite margins to monzonite plugs are interpreted to indicate that the diorite is the oldest phase of the Premier suite (Fig. 3). In the northern Mitchell valley, Premier suite syenite cuts monzonite and monzonite cuts diorite in drill core. Monzonite and syenite intrusions are cut in drill core by the Sulphurets suite diorite and related stockwork and alteration in the Iron Cap area. The Sulphurets suite, consisting of diorite to monzonite porphyry, are fine to medium grained. The Sulphurets suite is a partial host to all porphyry deposits in the district and were emplaced before, during, and after mineralization. Current geochronological data (Table 1) and cross cutting relationships suggest that the Premier suite magmatism preceded, and possibly overlapped with, the Sulphurets suite.

3.3. Structure

The Kerr, Sulphurets, Snowfield, and Iron Cap porphyry deposits are in the footwall of the Sulphurets fault (Fig. 3.), an east-vergent thrust that marks the eastern margin of the McTagg anticlinorium (Fig. 2). Both of these regional structures are interpreted to be kinematically linked to the Skeena fold and thrust belt (Kirkham and Margolis, 1995). The Mitchell thrust fault is a prominent splay of the Sulphurets thrust that separates the Snowfield and Iron Cap zones in its hanging wall from the Mitchell zone in its footwall (e.g., Savell and Threlkeld, 2013; Nelson and Kyba, 2014). Rocks in the Sulphurets area have been affected by folding, faulting, penetrative cleavage formation, and low-grade regional metamorphism (Kirkham, 1963; Henderson et al., 1992; Margolis, 1993). Beds in the

Table 1. Radiometric ages for Mitchell intrusions and related molybdenite mineralization in the Sulphurets district (¹laser ablation, ²TIMS).

Sub-district	Location	Stage	Suite	Unit	Sample	Method	Age	+	-	Reference
Brucejack	Bridge zone	-	-	hornblende porphyritic diorite	93-PL-185	U-Pb zircon ²	182.1	4.8	14.2	Lewis et al., 2001
Brucejack	Bridge zone	-	-	post-mineral mafic dike	-	U-Pb zircon ¹	182.7	1	1	Pretium Resources, 2013
Brucejack	south of Hanging Glacier	-	-	k-feldspar megacrystic dike	KQ-90-152	U-Pb zircon ²	188	0.5	0.5	McNicoll and Kirkham, in Kirkham and Margolis, 1995
Snowfield	east of Snowfield	post-3	-	k-feldspar megacrystic plagioclase-hornblende porphyry	S238	U-Pb zircon ²	189.6	2.2	2.2	Margolis, 1993
Mitchell	423312E 6265278N	1	Sulphurets	hornblende-plagioclase diorite porphyry	GF-13-02	U-Pb zircon ¹	189.9	2.8	2.8	this study
Brucejack	Bridge zone	-	n/a	molybdenite in vein	-	Re-Os	190.2	0.8	0.8	Pretium Resources, 2013
Mitchell	DDH M-10-116, 214.6 m	2	n/a	molybdenite in vein	M-10-116	Re-Os	190.3	0.8	0.8	this study
Brucejack	west of Hanging Glacier	-	Sulphurets	albite-hornblende porphyry	KQ-90-154C	Pb-Pb	191.4	5.3	5.3	Mortensen and Kirkham, in Kirkham and Margolis, 1995
Brucejack	Bridge zone (DDH SU-151)	-	n/a	molybdenite in vein	-	Re-Os	191.5	0.8	0.8	Pretium website, 2013
Sulphurets	Montgomery (Main Copper)	-	Premier	feldspar porphyry, monzonite to syenite	-	U-Pb zircon ²	191.8	6.5	1	Macdonald, in Kirkham and Margolis, 1995
Mitchell	DDH M-07-49, 320 m	2	Sulphurets	hornblende-plagioclase diorite porphyry	M-07-49	U-Pb zircon ¹	192.2	2.8	2.8	this study
Mitchell	southwest of Mitchell Glacier	pre-1	Premier	quartz syenite	S462	U-Pb zircon ²	192.7	5.4	3.6	Margolis, 1993
Mitchell	North of Mitchell glacier	pre-1	Premier	trachytoid syenite to aplitic granite porphyry	KQ-89-890/90A	U-Pb zircon ²	193.9	0.5	0.5	Mortensen and Kirkham, in Kirkham and Margolis, 1995
Brucejack	south of Hanging Glacier	-	Sulphurets	altered plagioclase-hornblende porphyry	KQ-90-151A	U-Pb zircon ²	194	1	1	McNicoll and Kirkham, in Kirkham and Margolis, 1995
Brucejack	west of West zone	-	-	k-feldspar megacrystic porphyry	93-PL-187	U-Pb zircon ²	194	3.7	0.6	Lewis et al., 2001
Kerr	Kerr deposit	-	-	k-feldspar megacrystic, plagioclase-hornblende porphyry	00-lskut	U-Pb zircon ²	195	1.5	1.5	Bridge, 1993
Mitchell	DDH M-11-123, 621 m	1	Sulphurets	diorite porphyry	M-11-123	U-Pb zircon ¹	196	2.9	2.9	this study
Sulphurets	Raewyn zone	-	Premier	altered quartz monzonite	-	U-Pb zircon ²	196	17	32	Macdonald, in Kirkham and Margolis, 1995
Kerr	western Kerr deposit	-	-	syenodiorite, symmineral	Iskut-lapp	U-Pb zircon ²	197	3	3	Bridge, 1993

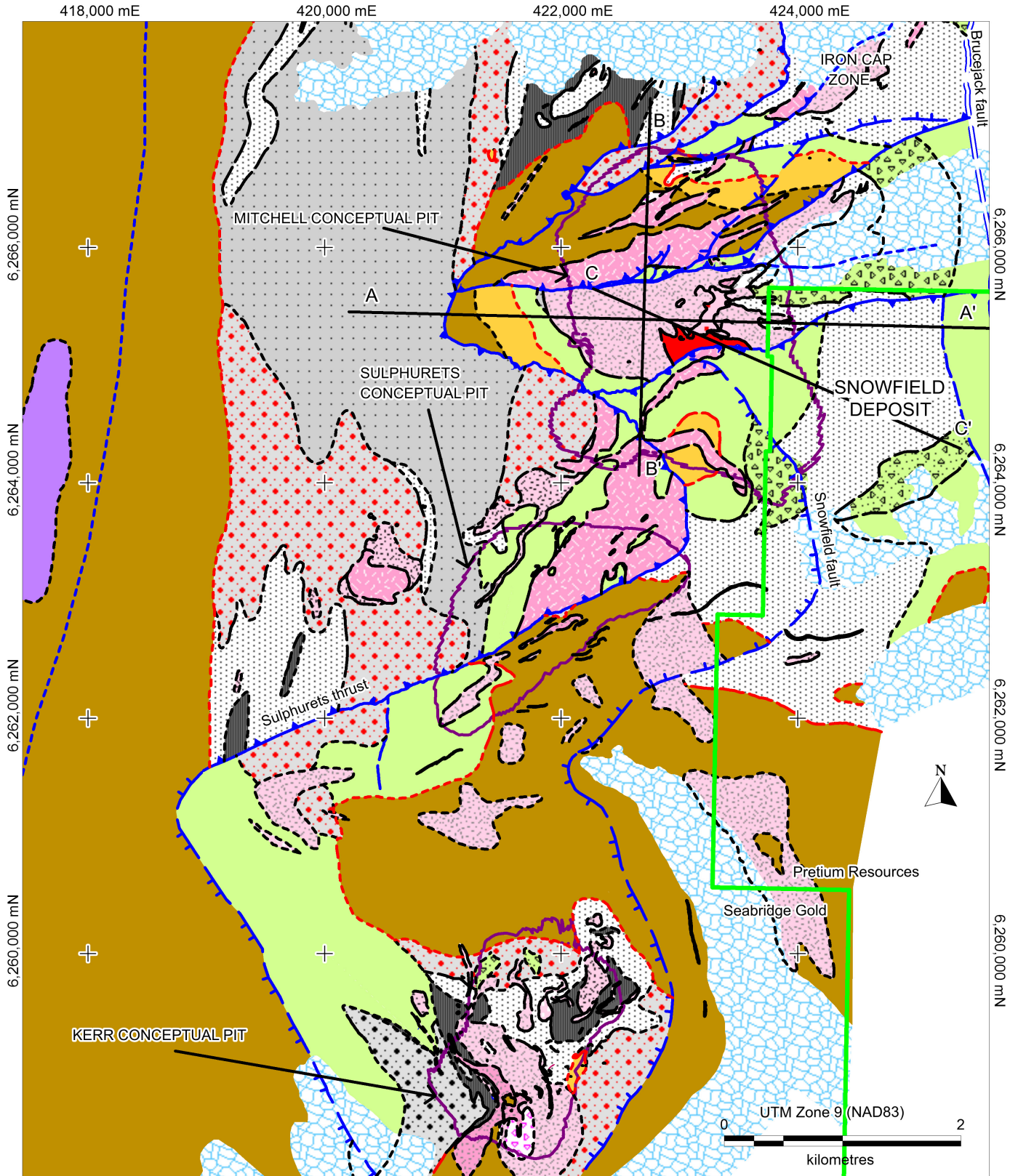


Fig. 3. Geology of the KSM property, showing the conceptual pit boundaries for Mitchell, Sulphurets and Kerr and the Snowfield and Iron Cap zones. For section A-A' refer to Figure 7a, for section B-B' refer to Figure 7b and for section C-C' refer to Figure 23. For lithology legend refer to Figure 4.

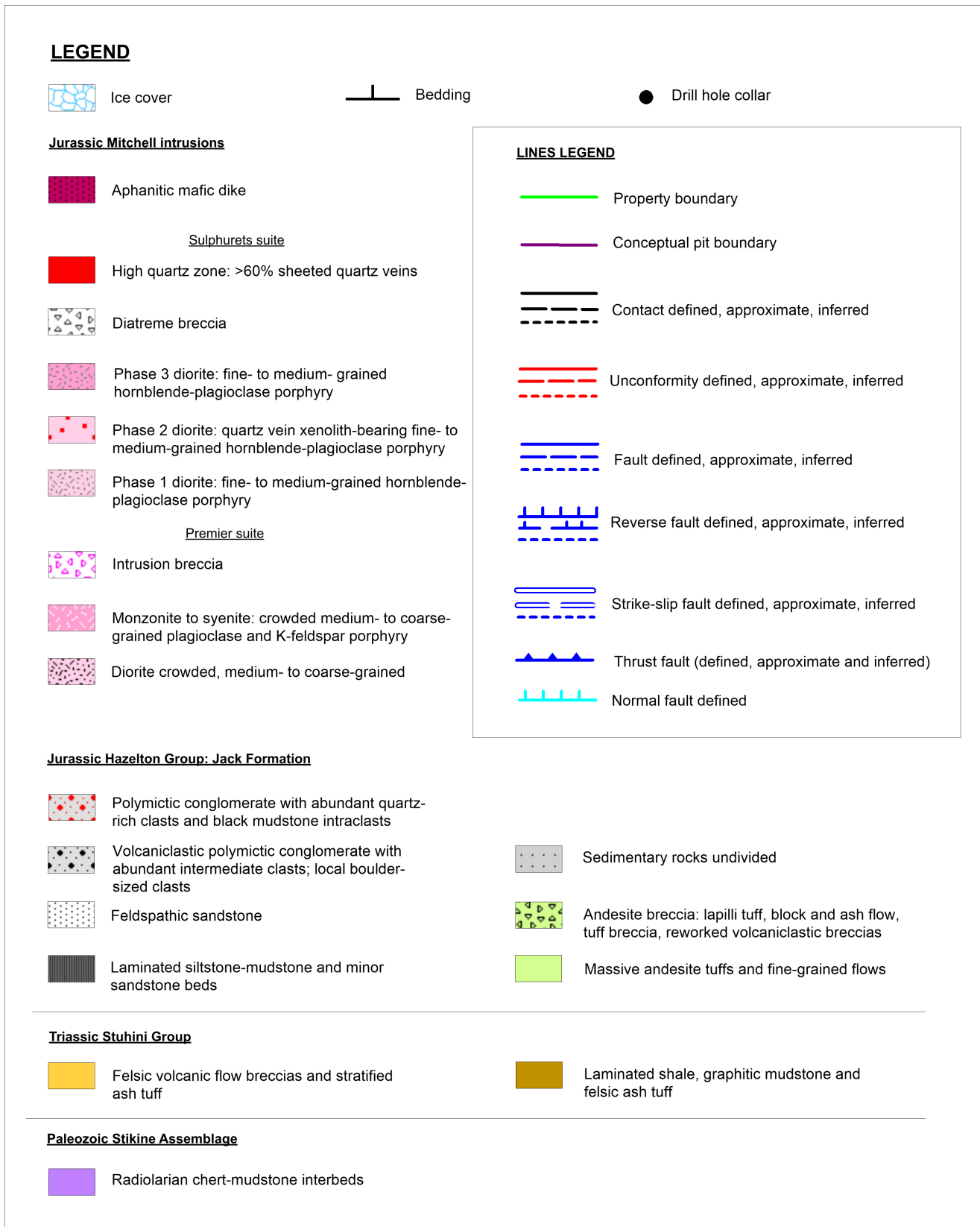


Fig. 4. Legend for Figures 3, 5, 7a, 7b, 8 and 21.

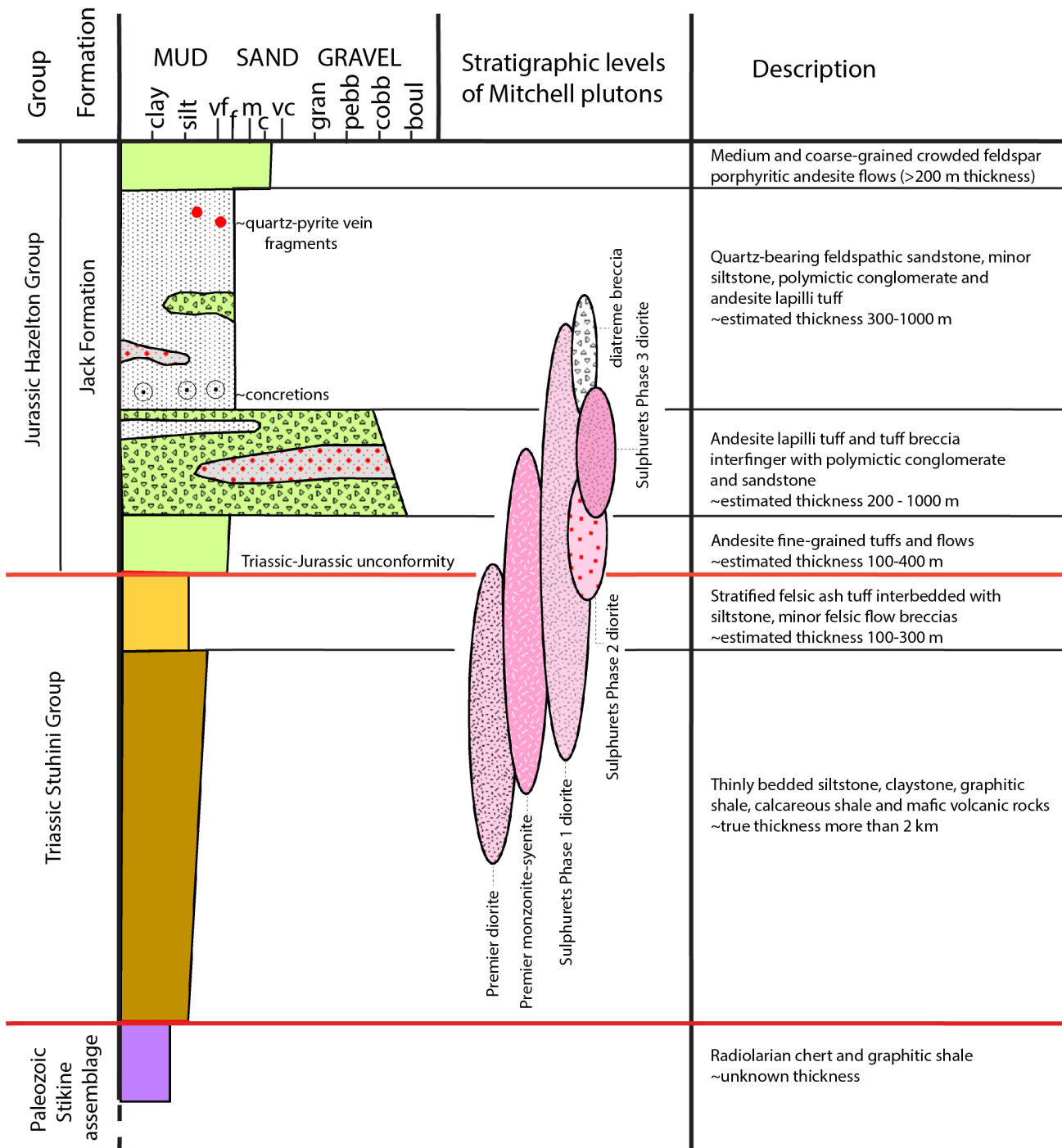


Fig. 5. Stratigraphy of the Mitchell-Snowfield area. For lithology refer to Figure 4.

district are generally north striking with moderate to steep dips and have been deformed into upright buckle folds, also related to Skeena fold and thrust belt deformation (Kirkham and Margolis, 1995). Two fold geometries are documented in the district: 1) north-northwest-plunging buckle folds with a related axial planar cleavage (Bridge, 1993; Kramer, 2014); and 2) west-plunging buckle folds, with a variably developed steep, north-dipping pressure solution cleavage (Kirkham,

1963; Margolis, 1993; this study). Although Margolis (1993) suggested that east-west striking cleavage in the Mitchell-Snowfield area may have developed as a post-emplacment fabric in the Jurassic, orthogonal fold trends in the Brucejack area may record progressive mid-Cretaceous deformation (C. Greig, pers. comm., 2014). Altered rocks at Kerr, Mitchell, Snowfield and Brucejack in particular are characterized by a strong pervasive pressure solution cleavage, folded veins, and

5-70% flattening compared to Sulphurets and Iron Cap, which have poorly developed deformation fabrics. Kirkham (1963) directly correlated cleavage development, degree of alteration, and abundance of micaceous minerals.

3.4. Mineralization

The Sulphurets district contains five undeveloped porphyry deposits (Kerr, Sulphurets, Snowfield, Mitchell and Iron Cap) and the high-grade epithermal Brucejack deposit (Fig. 2) with compliant estimates of mineral reserves and resources. Seabridge Gold Inc. claims cover the KSM property (Kerr, Sulphurets, Mitchell, and Iron Cap); Pretium Resources Inc. claims cover the Snowfield and Brucejack deposits. At surface, the Kerr deposit is hosted by Stuhini Group volcanosedimentary rocks, Jack Formation sandstone, and Sulphurets plutons; at depths of 0.5-1 km, it is intrusion hosted. The Sulphurets deposit is a tabular-shaped, northwest dipping ore body hosted in Jack Formation sandstone, andesite volcanic rocks, and subordinate Sulphurets suite monzodiorite to diorite dikes and sills. The Iron Cap and Snowfield deposits are hosted by Jack Formation sandstone, interfingering andesite volcanoclastic rocks, and Sulphurets suite intrusions.

The Mitchell deposit is largely hosted in Sulphurets suite diorite stocks. It lies in the footwall of the Mitchell thrust, and is considered equivalent to the Snowfield deposit which, in the hanging wall of the Mitchell thrust, is offset ca. 1.6 km to the southeast (Savell and Threlkeld, 2013). The KSM deposits have a measured and indicated resource of 2.78 billion tonnes at 0.55 g/t Au, 0.21% Cu, 2.9 g/t Ag and 55 ppm Mo (0.5 g/t gold equivalent cut off; Seabridge Gold, 2014). The Snowfield deposit hosts an additional measured and indicated resource of 1.37 billion tonnes at 0.59 g/t Au, 1.72 g/t Ag, 0.10% Cu and 85.5 ppm Mo (0.3 g/t gold equivalent cut off; Pretium Resources, 2011). The high-grade Valley of the Kings deposit (Brucejack project) contains a measured and indicated resource of 15.3 million tonnes at 17.6 g/t gold and 14.3 g/t Ag (5 g/t gold equivalent cut off; Pretium Resources, 2014).

The Snowfield deposit is underlain by andesite flow breccias and interbedded volcanoclastic arenite (Margolis, 1993) that host most of the mineralization. These rocks are intruded by pre-mineralization Sulphurets suite diorite and Premier suite quartz-syenite (192.7 ± 5.4 - 3.5 Ma; U-Pb, zircon; Margolis, 1993). Mineralization at Snowfield is divided into four stages (Margolis, 1993): Stage-1) deep, chalcopyrite-bearing potassic alteration flanked by propylitic alteration and Cu-Au enriched quartz-stockwork; Stage-2) high-level quartz-sericite-pyrite-chlorite-molybdenite-tourmaline; Stage-3) high-level advanced argillic alteration and deeper massive pyrite veins containing Bi-Te-Sn; and Stage-4) predominantly high-level, gold-rich vein and disseminated mineralization enriched in Ag-Pb-Zn-Ba-Sb-Hg-Cd-Te. Herein we adopt the Margolis (1993) scheme for the Mitchell deposit. Nelson and Kyba (2014) assigned quartz-rich arenites in the Snowfield area to the Jack Formation. Polymictic Jack Formation conglomerate outcrops west of the

Snowfield alteration zone (Nelson and Kyba, 2014). Argillic-altered sandstones in the upper part of the Jack Formation in the Snowfield area contain pebbles of banded quartz-pyrite vein fragments (Fig. 6a), indicating predepositional mineralization. Sulphurets suite porphyry plugs (Nelson and Kyba, 2014) contain Jack Formation sandstone xenoliths indicating that intrusion followed sedimentation. However, the Sulphurets suite porphyry is overprinted by alteration and mineralization (Margolis, 1993) and also contains clasts of chalcopyrite-bearing quartz veins (Margolis, 1993). In short, the mineralizing system appears to have been active before, during, and after deposition of the Jack Formation.

4. The Mitchell deposit

The Mitchell deposit is centred around a dense cluster of Mitchell porphyry diorites that cut the Stuhini Group and basal Hazelton Group (Jack Formation, Figs. 5, 8). Three pulses of Sulphurets suite diorite form a crudely elliptical 2 x 1 km outcrop with sills and dikes extending to the east. Multiple stocks of uniform medium-grained hornblende-plagioclase porphyritic diorite grade into coarse-grained porphyritic K-feldspar-hornblende-plagioclase diorite at depth (Figs. 7a, b). The deposit is characterized by episodic intrusion, stockwork and cannibalization of previously emplaced diorite and stockwork into later-stage intrusion breccias and diatremes. Deeper-level potassic and transitional potassic alteration in the western part of the map area grade into higher-level intermediate argillic and chloritic alteration in the central part which, in turn, grades to phyllic and clay alteration farther east. This alteration pattern is flanked by propylitic and albitic alteration that together with core alteration assemblages define a >4 km diameter alteration halo that is truncated by the Sulphurets thrust to the west and by the Brucejack fault to the east.

4.1. Lithologic units

4.1.1. Stuhini Group (Triassic)

The Stuhini Group is the oldest unit exposed in the Mitchell area (Fig. 8). The most abundant lithologies are cm-scale bedded siltstone, graphitic shales and less common calcareous mudstones intersected in drill core. Lesser amounts of dolostone and limestone are identified in drill core in the Mitchell mineralized zone (Hansley, 2008) and are of unknown thickness and extent. A unit of rhythmically bedded felsic tuff and siltstone assigned to Stuhini Group was intersected in drill core (Fig. 6b) in the western part of the map area, beneath the Mitchell thrust. Similar rocks outcrop north and south of the Mitchell zone above the Mitchell thrust fault (Fig. 8), and the unit appears to be >200 m thick. In the northwestern Mitchell valley, Jack Formation conglomerates contain clasts of a quartz-feldspar porphyritic flow breccia that were likely derived from an identical breccia body immediately beneath the unconformity (Fig. 6c). Ubiquitous felsic clasts in the Jack Formation were likely derived from similar rocks (J. Nelson, pers. comm., 2014).

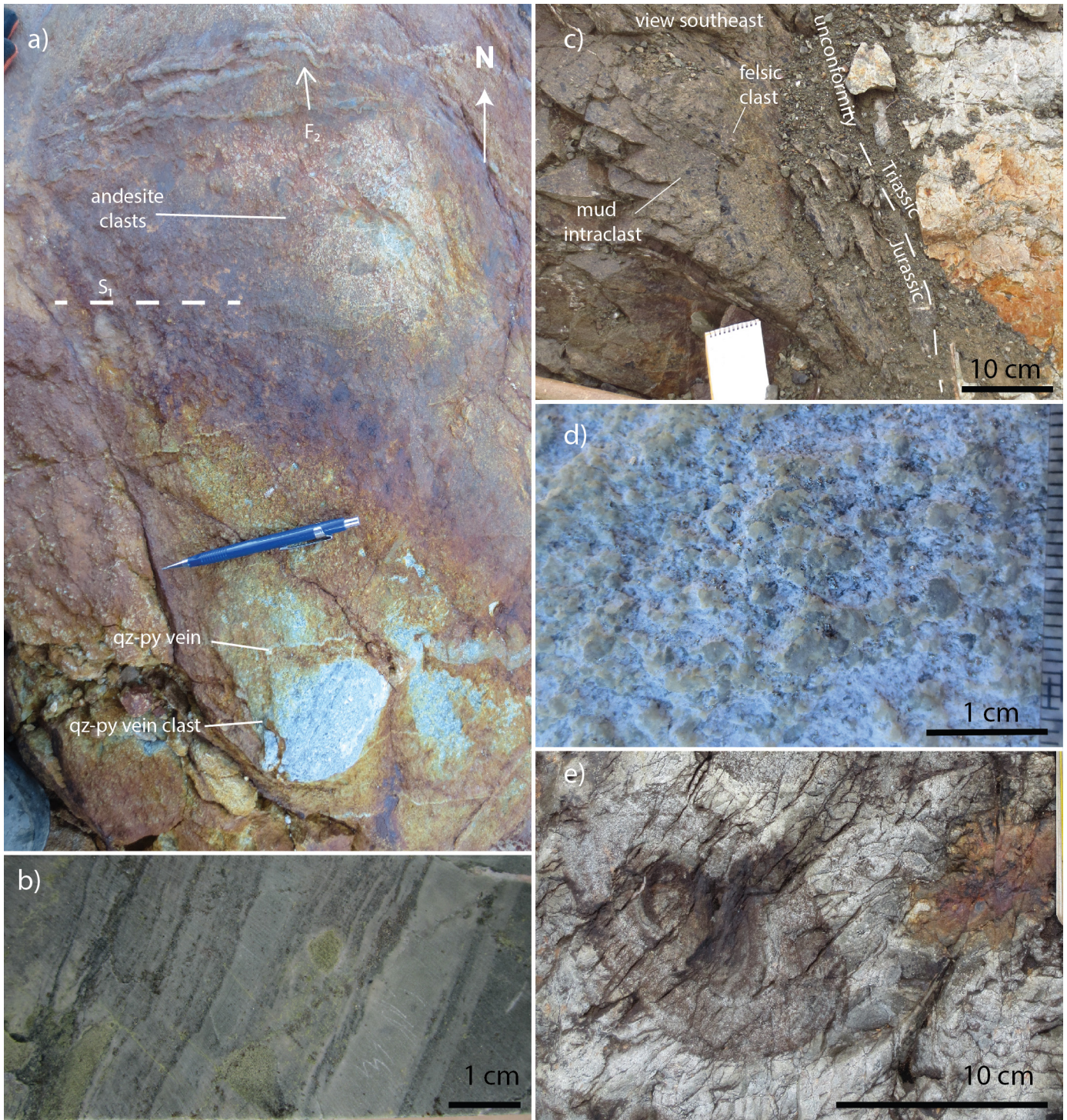


Fig. 6. Mitchell zone and surrounding area rocks. **a)** Jack Formation conglomeratic sandstone in the Snowfield zone with andesite and quartz-pyrite vein clasts. S_1 and veins folded by F_2 , 424583 E, 6264244 N. **b)** Pale Stuhini Group felsic ash tuff interbedded with siltstone (drill core, M-07-42, 348.7 m). **c)** Jack Formation conglomerate contains felsic flow breccia clasts derived from subjacent Stuhini Group, 421431 E, 6266817 N. **d)** Phyllic- and clay-altered Jack Formation feldspathic sandstone of the Mitchell zone, 424861 E 6265572 N. **e)** Elliptical concretionary structure in Jack Formation sandstone with concentric banding defined by albite-chlorite-chalcopyrite-pyrite, 424475 E 6266436 N.

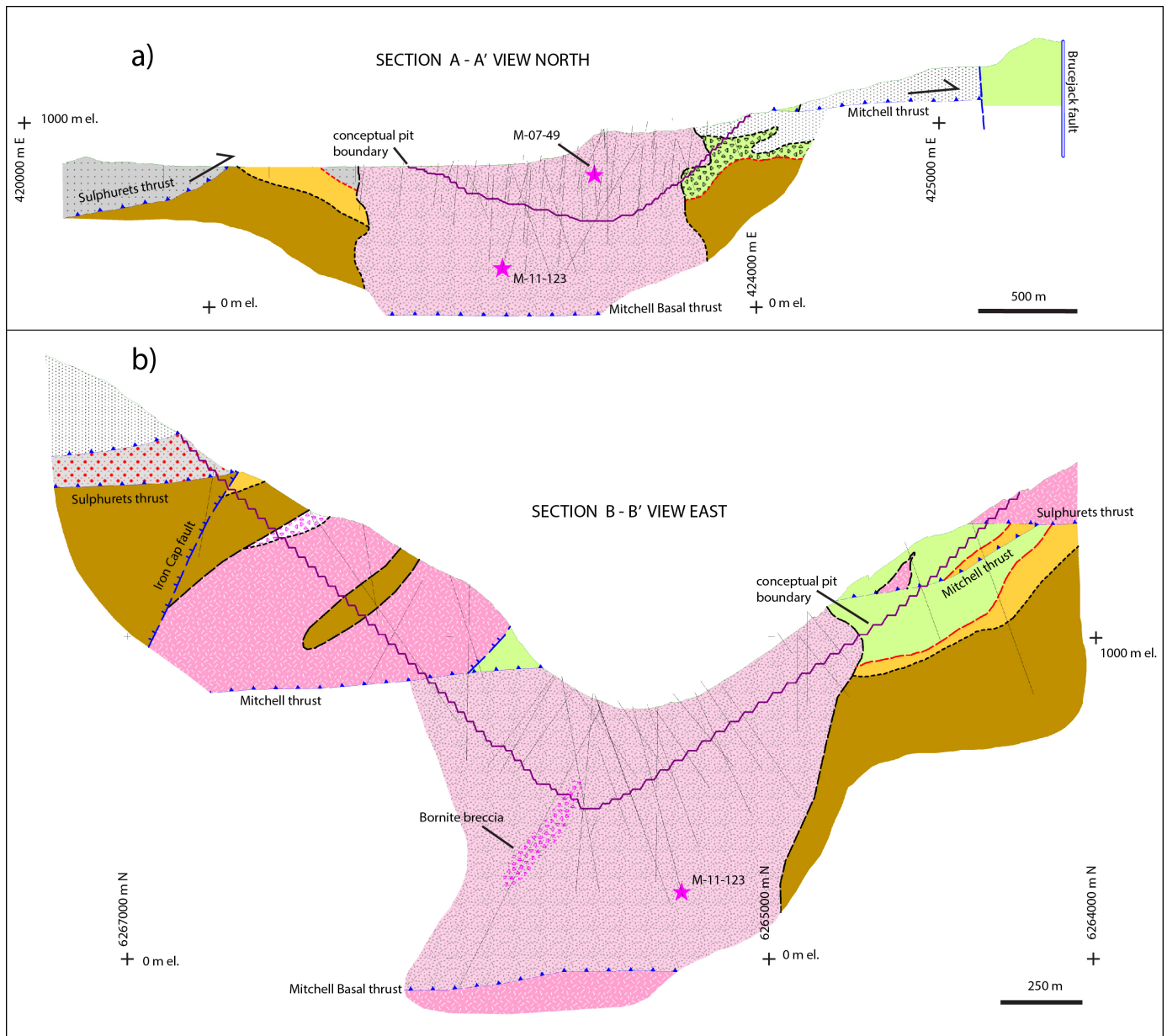


Fig. 7. Cross sections across KSM property (see Fig. 3 for locations): **a)** A-A' east-west, **b)** B-B' north-south. For lithology legend, refer to Figure 4.

4.1.2. Hazelton Group (Late Triassic to Middle Jurassic)

Beneath the Mitchell thrust fault east of the Mitchell deposit (Fig. 8), the Jack Formation is represented by a unit of massive feldspathic sandstone (Fig. 6d). The sandstone contains 10-45% quartz and 50-70% feldspar and is typically very fine grained to fine grained, but with rare granule fragments. The unit is 300 m to 1 km thick and has gradational contacts with conglomerate and andesite lapilli tuff. Rarely, the sandstones contain lenses of conglomerate up to 10 m thick with felsic volcanic, black chert and intermediate volcanic clasts in a sandstone matrix. In the northeastern Mitchell zone, bedding in the lower part of the sandstone unit is locally defined by high concentrations of concretionary structures with concentric

bands of chalcopyrite-pyrite-chlorite-albite (Fig. 6e). Some concretions contain small amounts of carbonate. The intensity of hydrothermal minerals in concretionary structures relates to intensity of pervasive and mottled chalcopyrite-pyrite-chlorite-albite in sandstone and to the proximity to Sulphurets dikes. If the concretionary structures are a product of diagenesis that contained carbonate cement, then mineralization post-dates both sandstone deposition and diagenesis.

Jack Formation sandstone is intruded by pre- to post-mineral Sulphurets diorite and is intensely altered to albite, quartz-sericite-pyrite and muscovite-illite in all outcrops beneath the Mitchell thrust fault. Alteration is characterized by partial to complete replacement of feldspar and interstitial carbonate by

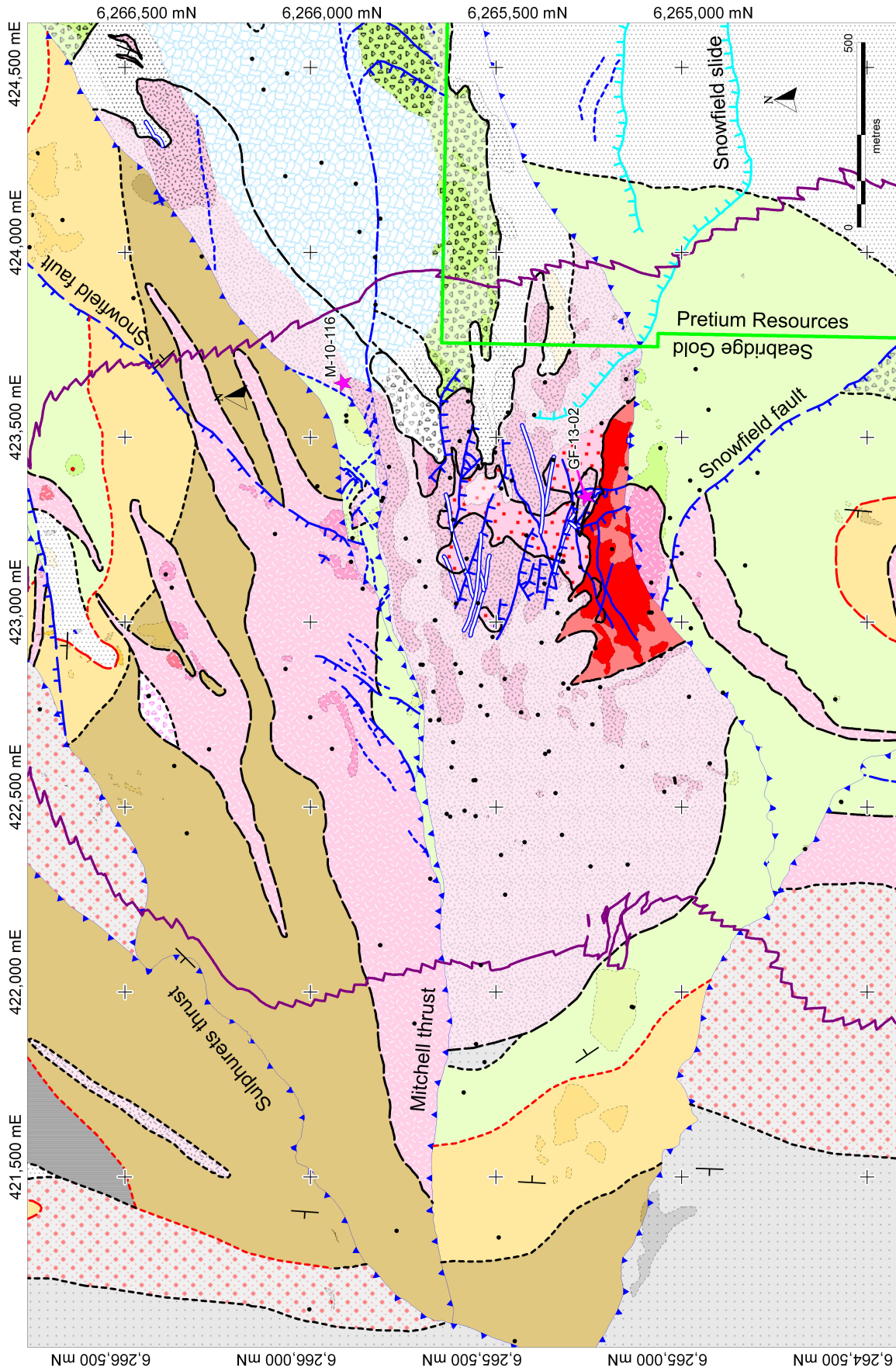


Fig. 8. Geology of the Mitchell zone and surrounding area. Geochronologic sample GF-13-02 from outcrop, M-10-116 from drill core. For legend, refer to Figure 4.

hydrothermal minerals. Quartz grains in altered sandstone are subrounded to angular and fractures in grains are commonly filled with pyrite and chalcopyrite.

Andesite volcanic rocks in the Mitchell zone outcrop beneath the Mitchell thrust fault east of the Mitchell intrusions (Fig. 8). They comprise three general types that are broadly laterally equivalent: 1) lapilli-sized breccia; 2) tuff-breccia; and 3) feldspar-phyric flows. The breccia are well sorted, massive, and contain abundant (60-85%) 1-2 cm porphyritic juvenile clasts with aspect ratios that range from 1:1 to 2:1 (Fig. 9a). Clast sizes tend to be uniform within individual layers, and many of the clasts have concavo-convex shapes and margins with flame-like projections. The breccias interfinger with sandstone layers and locally contain a sandstone matrix. The deposits are interpreted to record subaqueous phreatomagmatic volcanic eruptions, as indicated by the porphyritic textures and irregular clast boundaries, coeval with sandstone sedimentation. Andesite tuff breccia deposits contain poorly sorted, 50-80%, angular, porphyritic clasts that range from ~1 cm to more than 1 m in a massive tuffaceous matrix (Fig. 9b). They display local stratification and rare sigmoidal shaped fiamme fragments. Fragments typically have aspect ratios of 1:1 to 5:1. Sections with >1 m clast sizes are interpreted to be near-vent deposits. The deposits are interpreted to be block and ash flows due to their poor sorting, tuffaceous matrix and the angular, large monolithic andesite clasts.

Andesite flows and flow breccias outcrop in the most easterly Mitchell zone beneath the Mitchell thrust and west of the Brucejack fault (Fig. 8), where they probably represent the highest parts of the section. Fine-grained plagioclase-hornblende-phyric flows near the sandstone contact grade into overlying crowded, coarse-grained (up to 1 cm), feldspar-phyric flows. A lava tube, ca. 2 m in diameter, outcrops in the transition between fine- and coarse-grained intermediate flow sequences. The tube is defined by concentric flow banding that is truncated by a subhorizontal erosional surface and overlain locally by a coherent andesite flow and flow breccia (Fig. 9c).

The andesites host stockwork and disseminated mineralization and are cut by Sulphurets suite diorite intrusions. The andesites are interpreted to be coeval with the Premier suite intrusions because: 1) of their stratigraphic position within the basal Hazelton Group; 2) of their spatial association with Premier intrusions; and 3) at Snowfield they contain hypabyssal syenite clasts with a pink K-feldspar matrix (J. Nelson, pers. comm., 2013). Above the Mitchell thrust, offset equivalents of the andesite strata of the Mitchell zone are locally cut by Premier suite syenite and monzonite in drill core and Sulphurets suite diorite in outcrop (Fig. 8).

4.1.3. Premier intrusive suite

Premier suite intrusions outcrop in the immediate hanging wall of the Mitchell thrust fault (Figs. 8, 7b). Premier suite plutons are characteristically phaneritic with crowded oscillatory zoned plagioclase and common pink or maroon K-feldspar phenocrysts (Figs. 10a, b). Dioritic varieties are

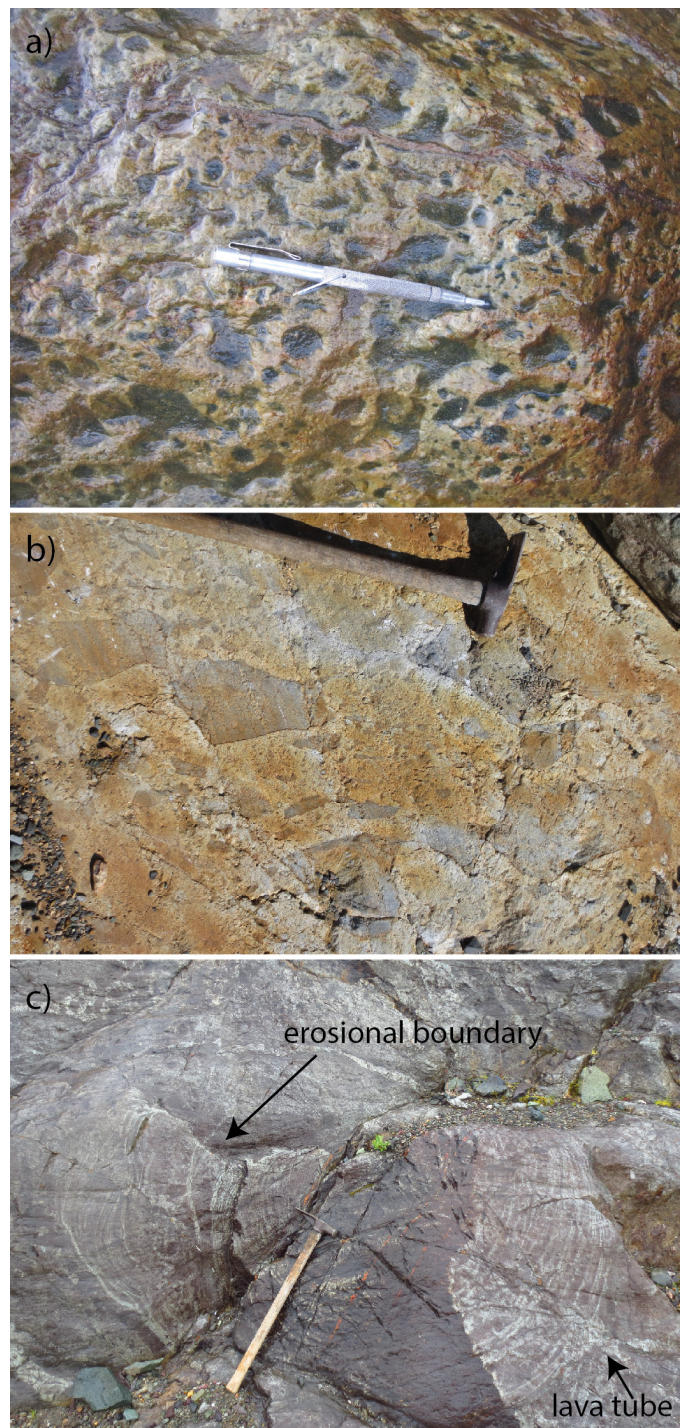


Fig. 9. Mitchell zone Jack Formation andesite. **a)** Chlorite and quartz altered phreatomagmatic andesite lapilli tuff, 424000 E, 6265584 N. **b)** Andesite block breccia, 424950 E, 6265755 N. **c)** Lava tube with concentric bands cut by overlying andesite flow breccia, 424874 E, 6266646 N.

crowded biotite-pyroxene-hornblende-plagioclase phyric, medium- to coarse-grained porphyries that outcrop in the southwestern Mitchell valley above the Sulphurets thrust fault (Fig. 3). Monzonite varieties are commonly coarse grained, crowded with oscillatory zoned plagioclase, pink K-feldspar

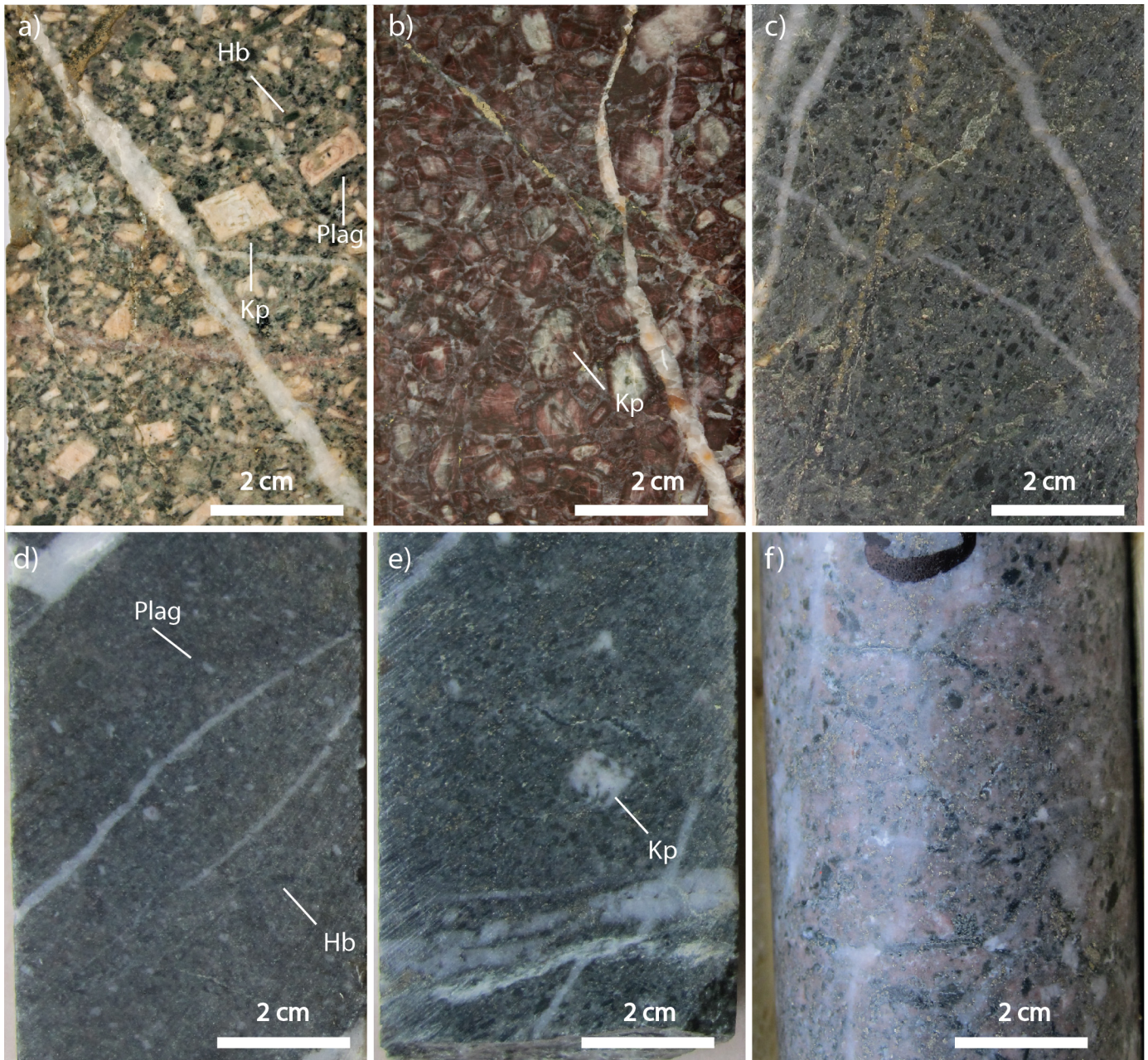


Fig. 10. Mitchell intrusions; Premier and Sulphurets suites (Jurassic). **a)** Premier suite; coarse-grained, crowded monzonite porphyry. Hb- hornblende; Plag- plagioclase; Kp- K-feldspar. Drill core M-06-23, 54 m. **b)** Premier suite; red hematite dusted coarse-grained, syenite. Plag- plagioclase; Kp- K-feldspar. Drill core M-12-129, 895 m. **c)** Sulphurets suite; Phase 1 diorite with chloritized hornblende and plagioclase phenocrysts. Drill core M-07-58, 690.5m. **d)** Sulphurets suite; Phase 1 medium-grained diorite; Hb- hornblende; Plag- plagioclase. Drill core M-07-42, 50 m. **e)** Sulphurets suite; Phase 1 bimodal porphyry diorite contains 1% coarse-grained K-feldspar (Kp) phenocrysts in a hornblende-plagioclase, medium-grained diorite porphyry. Drill core M-07-25, 456.6m. **f)** Phase 1 diorite with k-feldspar-altered groundmass and chlorite-altered mafic phenocrysts. Drill core M-11-126, 336.5 m.

phenocrysts up to 2 cm, hornblende up to 1 cm, biotite and trace quartz phenocrysts (Fig. 10a). Syenitic varieties (Fig. 10b) are commonly maroon to red, contain from 40-65% perthitic K-feldspar phenocrysts, oscillatory zoned plagioclase phenocrysts, local quartz phenocrysts, and lack mafic primary minerals (Kirkham, 1963; Simpson, 1983).

4.1.4. Sulphurets intrusive suite and related breccia bodies

Sulphurets suite plutons in the Mitchell deposit are diorite in composition. Compared to the Premier suite diorite, they are more uniform in texture and composition, and are notably finer grained and less crowded (Figs. 10c-d). Based on field observations, we distinguish three phases of diorite. Phase 1 includes diorite in contact with country rock and Phase 2 is a

plug that crosscuts Phase 1 rocks and contains quartz-pyrite-chalcopyrite veins as xenoliths. A breccia body and small breccia dikes cut Phase 2 rocks but are cut by a small Phase 3 plug.

4.1.4.1. Phase 1 diorite

Phase 1 diorite is the most voluminous of the three Sulphurets intrusions. It cuts bedded sedimentary rocks of the Stuhini Group and both cuts and interfingers with Jack Formation sandstone and andesite breccia (Fig. 8). The margins of the diorite contain xenoliths of sedimentary rocks. The country rock adjacent to the intrusions has albite alteration and local skarn alteration mineralogy (see below). Phase 1 diorite is a partial host to the high quartz zone (Fig. 8) near the southern contact area and is interpreted to have been emplaced prior to or possibly synchronous with the high quartz zone that is cut by Phase 2 diorite. (Fig. 8). Phase 1 diorite is remarkably homogeneous in composition and texture and is characterized by partial to complete hydrothermal replacement of plagioclase and replacement of hornblende phenocrysts (Figs. 10c, e, f). A narrow diorite sill intersected in drill core along the western margin of the Mitchell zone is relatively unaltered and provides primary texture information (Fig. 10d). This sill contains 20-30% plagioclase (An_{10} - An_{20}) phenocrysts (up to 3 mm) 1-10% K-feldspar (up to 1 mm), 5% hornblende phenocrysts (up to 3 mm), trace biotite (ca. 1 mm) and trace apatite. At depth, diorite contains up to 1% K-feldspar oikocrysts 1-1.5 cm in diameter in local coarser intervals (Fig. 10e). Inclusions in the K-feldspar oikocryst include 20% anorthite, 5% hornblende, 1% clinopyroxene and trace garnet. Where Phase 1 diorite is cut by veins with relatively sharp boundaries, we infer emplacement before mineralization. Where mineralized veins in the diorite are disarticulated, fluidal shaped, and irregular, which suggests incomplete diorite crystallization, we infer synmineralization emplacement.

4.1.4.2. Phase 2 diorite

The Phase 2 intramineral diorite plug contains quartz vein xenoliths, cuts Phase 1 diorite and the high quartz zone (Fig. 11a) and occupies the core of the deposit (Fig. 8). It is distinguished on surface by a contact breccia, sparser (10-20%) quartz veins than Phase 1, and uniformly high concentrations of quartz vein xenoliths (Fig. 11b). Contacts between Phase 1 and Phase 2 are most clearly identified where Phase 2 rocks cut the high quartz zone, with quartz zone xenoliths in the contact breccia (Fig. 11a) and by internally stockworked Phase 1 diorite xenoliths (Fig. 11c). Elsewhere, contacts are inferred by transitions from higher to lower quartz stockwork coupled with an increase in quartz vein xenoliths.

4.1.4.3. Diatreme breccia

A ca. 100 x 300 m, northeast-trending complex breccia body interpreted to be the root zone of a diatreme breccia, outcrops in the northeastern Mitchell zone (Fig. 8). It cuts Phase 2 diorite on its southern margin, and cuts sandstone and andesite on its

southeastern margin, but is cut by Phase 3 diorite at its western margin where indistinct boundaries to xenoliths of the diatreme within Phase 3 diorite are interpreted to indicate an unlifted breccia at the time of Phase 3 magmatism (Fig. 11d). On the west, clast sizes are up to 20 cm in diameter, on the east clasts are generally <2 cm across. Clasts include: 1) andesite volcanic fragments that are 1-2 cm in diameter, fine-grained, porphyritic, and angular (Figs. 12a, b); 2) quartz-rich sandstones that are subrounded and <3 mm in diameter; 3) porphyritic diorite(?), that display amoeboid shapes and 2-6 cm in diameter; 4) quartz-pyrite±chalcopyrite veins, 0.5-3 cm in diameter (Fig. 12b); and 5) mineralized quartz stockworked diorite (Fig. 12a) that are subrounded and 2-20 cm in diameter. Concentrations of quartz stockworked diorite clasts can make up 80% of the rock in the western 'bone breccia' outcrop (Fig. 12a; see also Fig. 20 in Kyba and Nelson, 2014) but decrease eastward. Clasts of andesite or diorite are flattened to form local banding that is at an angle to the overprinting pervasive foliation (Fig. 12b). The breccia is overprinted by 1-5% quartz-chalcopyrite-molybdenite stockwork. Late quartz-pyrite stringers with tourmaline alteration halos are common, and tourmaline is locally in the groundmass. The groundmass displays weak chlorite and sericitic alteration, but subtle porphyritic textures in thin section suggest a magmatic origin.

We interpret that the breccia formed as a subvertical diatreme pipe that now plunges steeply to the west, and that the eastward decrease in clast sizes reflects increasing distance from source rocks. Cross-cutting relationships suggest that the pipe was emplaced during the waning stages of Phase 2 plutonism, and/or the early stages of Phase 3 plutonism. Emplacement of the diatreme pipe coincided with the waning of latest molybdenite-rich, porphyry-type mineralization and cessation of stockwork veining. The quartz stockwork dense 'bone breccia' outcrop is interpreted to be an intact root zone to the diatreme breccia that is penetrated by intrusion breccia dikes (see also Nelson and Kyba, 2014).

4.1.4.4. Intrusion breccia dikes

Small (20-50 cm wide; 2-20 m long) intrusion breccia dikes cut sandstone, Phase 1 and 2 diorite, and the diatreme breccia and they are cut by Phase 3 diorite. The dikes are distributed about the margins of and emanate from, Phase 3 diorite. Boundaries are commonly sharp and irregular, and dike traces anastomose. Where dikes cut sandstone, clasts of chert, rounded siliceous pebbles and angular mineralized quartz veins are in a tourmalinized porphyritic groundmass (Fig. 13c). Where dikes cut the diorite, clasts are predominantly quartz vein fragments and quartz stockworked diorite fragments. Where dikes cut the diatreme breccia, they contain clasts of quartz stockworked diorite, angular diorite(?) porphyry, and quartz veins in a tourmalinized groundmass. The clast compositions in these three examples appear to directly reflect cannibalization of the host lithologies. Breccia dikes are cut by pyrite-quartz veins with tourmaline halos and tourmaline is commonly observed in the groundmass of the dikes (Fig. 13c). A particularly notable

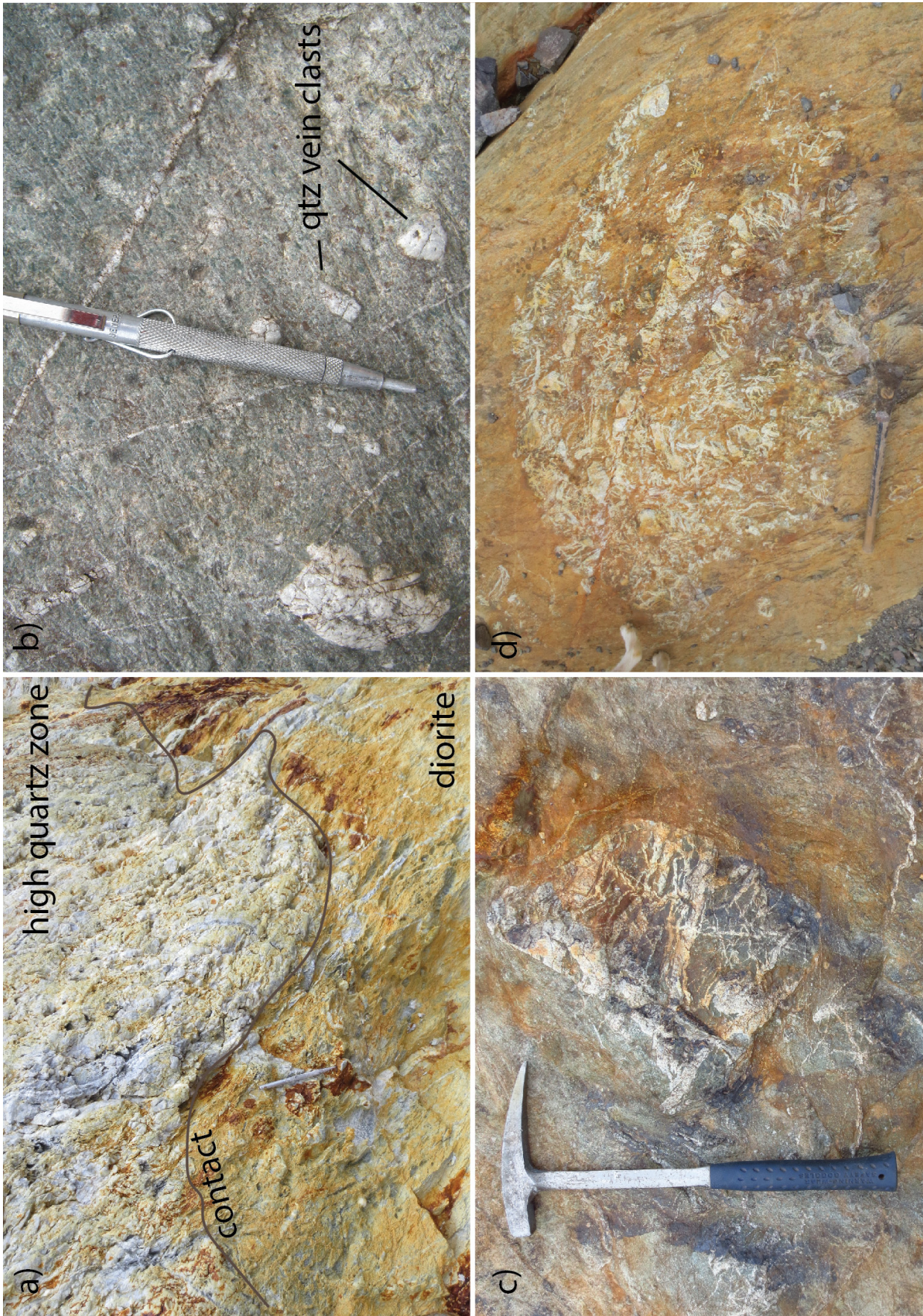


Fig. 11. Sulphurets suite diorite breccia. **a)** Contact between Phase 2 phyllic altered diorite and high quartz zone, 423353 E, 6265193 N. **b)** Angular quartz vein xenoliths in Phase 2 diorite, 422958 E, 6265505 N. **c)** Xenolith of Phase 1 diorite (with internal quartz stockwork veins abruptly truncated at clast boundary) in Phase 2 diorite, 423300 E, 6265575 N. **d)** Clast of diatreme breccia in Phase 3 diorite, 423391 E, 6265661 N.

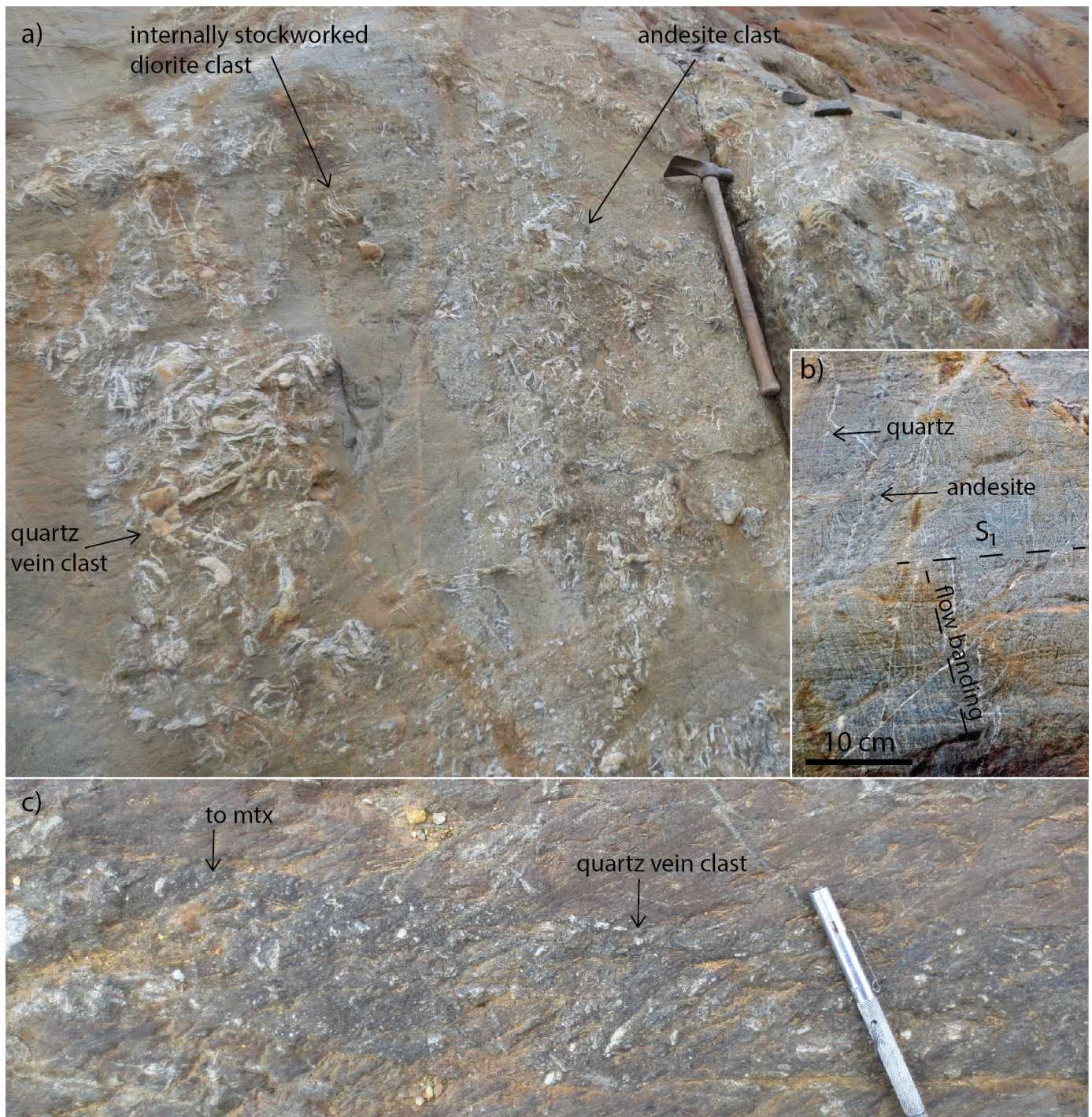


Fig. 12. Diatreme breccia and intrusion breccia dike in outcrop. **a)** Dense internally stockworked diorite clasts, quartz vein and andesite fragments 423469 E, 6265628 N. **b)** Irregular flow banding in the diatreme breccia is locally at a high angle to steeply dipping main cleavage (S_1), 423511 E, 6265640 N. **c)** Intrusion breccia dike with tourmalinized groundmass, containing quartz-chalcopyrite-pyrite vein clasts, 423575 E, 6265533 N.

3 m thick breccia dike that intrudes the diatreme breccia is cut by Phase 3 diorite. The breccia dikes are interpreted to have been emplaced during the early stages of Phase 3 diorite intrusion as they emanate from the Phase 3 plug and are locally cut by it.

4.1.4.5. Phase 3 diorite

A small (50 x 125 m) plug of Phase 3 diorite cuts the western end of the diatreme breccia (Fig. 8) and intrusion breccia dikes, and is overprinted only by minor quartz-pyrite-tourmaline stringers. The plug is most easily distinguished by a near lack (<1%) of quartz veins, and by abundant clasts of quartz

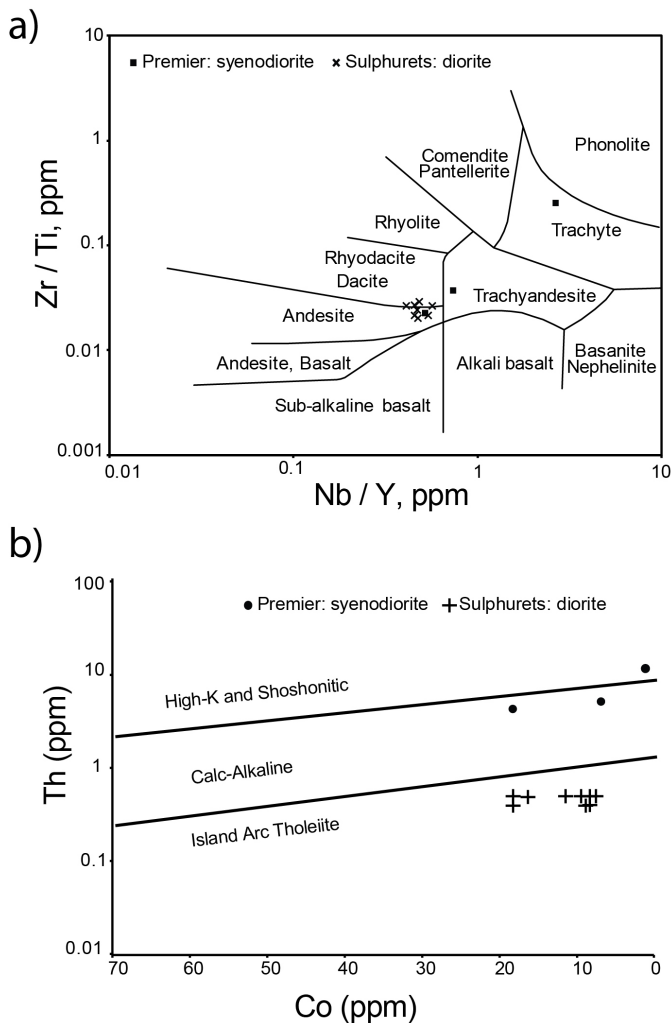


Fig. 13. Geochemistry of the Mitchell intrusions (Premier and Sulphurets suites). **a)** Zr/Ti vs Nb/Y diagram (Winchester and Floyd, 1977) and **b)** Th vs Co diagram (Hastie et al., 2007).

stockworked diorite (up to 20 cm), clasts of diatreme breccia (>1 m, Fig. 11c) and clasts of breccia dikes. The plug is assigned intermineral status because it post-dates Stage 2 stockwork and pre-dates Stage 3 pyrite stringers described below.

4.2. Geochemistry of the Premier and Sulphurets intrusions

On plots of immobile elements (Fig. 13a), most intrusions of the Mitchell deposit plot in the andesite (diorite) field, although some plugs border the dacite (monzonite) field. Compositions of the Premier and Sulphurets suites are comparable, although the younger phases of Premier magmatism trend toward the trachyte (syenite) fields. Kirkham (1963) attributed this compositional differentiation to fractional crystallization, with composite intrusions resulting from progressive crystallization from diorite to monzonite to syenite over time. The Premier and Sulphurets suites display separate trend lines on a Co versus Th plot (Fig. 13b), which shows the Premier to be more alkaline. Overlapping crystallization ages of the Premier and Sulphurets suites (Table 1) suggest that they may have been emplaced in separate but kindred crustal chambers.

4.3. Alteration

Adopting the alteration scheme developed for the Snowfield deposit by Margolis (1993), we recognize three stages of alteration in the Mitchell deposit (Table 2).

4.3.1. Stage 1

Stage 1 potassic alteration is characterized by equigranular textures and a simpler, less dense quartz vein stockwork in the western Mitchell zone (Fig. 14) and in the central, deeper regions of the drilled extents of the Mitchell intrusion. Secondary biotite, K-feldspar (Fig. 10f), magnetite, albite, anhydrite, chlorite, phengite are commonly preserved. The potassic assemblage transitions laterally and upwards (into stratified wall rocks) to transitional potassic, a calcite-epidote-chlorite distal propylitic (Fig. 6b) and hornfels alteration that contains epidote, albite, cordierite and carbonates, and quartz veins diminish in volume. The transitional potassic alteration (Fig. 14), characterized by quartz, chlorite, anhydrite, magnetite, biotite and several episodes of quartz stockwork veins, is outboard of the core potassic alteration zone and inboard of the propylitic zone. Here, fine, shreddy textures and rutile inclusions commonly observed in chlorite suggest that chlorite replaces some of the secondary biotite. Local zones of skarn mineral assemblages, including magnetite, diopside, zoisite, garnet and epidote occur, farther outboard in the hornfelsed host rocks.

Table 2. Summary of mineralization, alteration, vein and plutonic stages and phases.

Stage	Plutonism	Alteration	Mineralization	Veins	Age
1	Phase 1	potassic, transitional potassic, propylitic, albitic	Cu-Au core zone	5-95% by volume quartz-pyrite-chalcocopyrite veining, sheeted high quartz zone	196.0 ± 2.9 Ma - 190.3 ± 0.8 Ma
2	Phase 2	phyllic	Mo envelope, additional Cu-Au	<10% by volume quartz-pyrite-chalcocopyrite-molybdenite veining	190.3 ± 0.8 Ma
3	Phase 3	advanced argillic	n/a	massive pyrite veins	<190.3 ± 0.8 Ma
4	n/a	n/a	high grade Au-Ag-Cu-Pb-Zn	epithermal	185(?) Ma

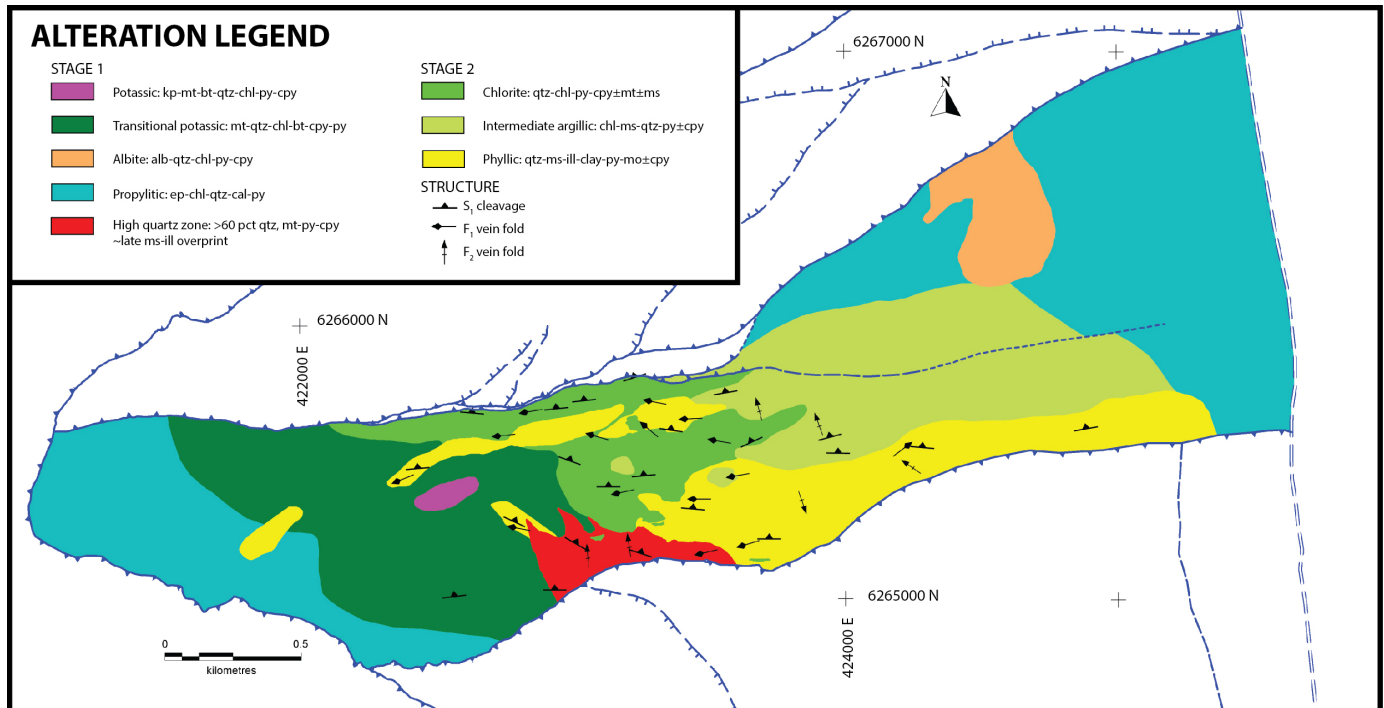


Fig. 14. Alteration map for the Mitchell zone. Alteration above the Mitchell thrust fault is not plotted.

4.3.2. Stage 2

Secondary phyllic alteration overprints the primary alteration (Fig. 14) and consists of quartz, sericite, illite, and chlorite accompanied by quartz stockwork veins (Figs. 9b, 11a). The degree of overprint ranges from spaced, metre scale, fracture-controlled replacement in deeper regions of the porphyry (observed in drill core), to pervasive overprint in the eastern and upper levels of the deposit. Intense phyllic alteration in the eastern Mitchell zone is defined by bleached to pale grey or yellow rocks entirely lacking in mafic minerals and magnetite (Fig. 6d).

4.3.3. Stage 3

Stage 3 advanced argillic alteration includes kaolinite, pyrophyllite and rutile in southeastern Mitchell zone. High pyrite concentrations are spatially associated with this alteration type, but lack significant gold and copper mineralization.

4.4. Vein paragenesis

Adopting the vein paragenesis scheme developed for the Snowfield deposit by Margolis (1993), Stage 1 veins comprise mm- to cm-scale stockwork to sheeted veins (Figs. 15a-c) that make up 5-95% of the host rock and are composed of chalcopyrite-pyrite-quartz±magnetite±K-feldspar±chlorite. The high quartz zone, formed during Stage 1, is characterized by 1-2 cm thick, sheeted quartz veins that strike east-northeast and dip steeply to the north (Fig. 15b). The high quartz zone is tabular in shape and grades into lower quartz vein abundance stockwork to the west. To the north, the high quartz zone is cut by Phase 2 diorite. In general, Stage 1 veins have uniform

mineralogy, lack alteration halos (Fig. 15c) and are part of a protracted stockwork event that overlapped with emplacement of Phase 1 diorite. At deeper levels Stage 1 stockwork displays diffuse boundaries and contain more magnetite and K-feldspar but are interpreted to be part of the same progressive stockwork event that is responsible for the vast majority of veins in the deposit. Stage 1 veins are temporally associated with early potassic and propylitic alterations (Margolis, 1993).

Stage 2 molybdenite-rich vein and stockwork bodies are distributed in a halo about the core copper-gold mineralized zone and are composed of quartz-pyrite-molybdenite±chalcopyrite±chlorite±sericite±fluorite±anhydrite. The veins are more typically stockwork-style and are not sheeted in the Mitchell zone. Molybdenite-bearing veins (Fig. 15d) are generally associated with smaller volumes of quartz veins compared to Stage 1 veins. Stage 2 veins are spatially distributed with phyllic alteration assemblages (Fig. 14). A bornite-bearing hydrothermal stockwork and breccia body intersected in drill core (Fig. 7b) is interpreted as Stage 2. The breccia body overprints Stage 1 stockwork and is cut by Stage 3 pyrite veins and a late, narrow diorite sill interpreted as Phase 3. The bornite breccia is interpreted to be up to ca. 100 m thick tabular to pipe-like body that plunges steeply to the north. Contact margins of the breccia contain clasts of Phase 1 quartz stockwork and diorite, and the core areas contain banded, stockwork and breccia textures with clasts and matrix composed of hydrothermal gangue and sulphide minerals. Clasts in the breccia are commonly lenticular and irregular and are interpreted to have been coeval with the matrix because the mineralogy of both is comparable. X-ray diffraction determinations of gangue and

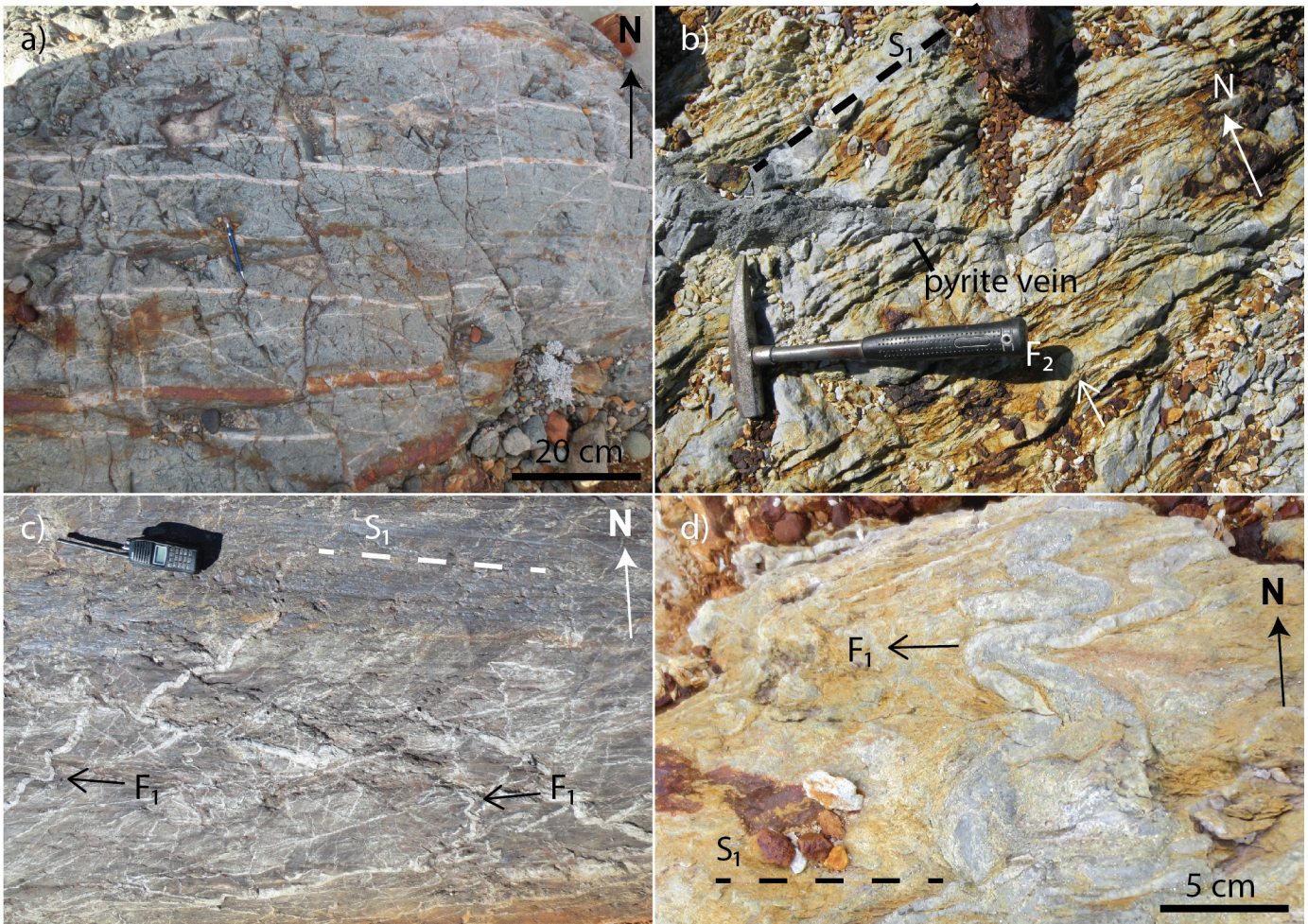


Fig. 15. Quartz stockwork and vein fold geometry in the Mitchell zone. **a)** Planar Stage 1 quartz-K-feldspar-magnetite-chalcopyrite veins in potassic altered diorite, 422532 E, 6265370 N. **b)** Sheeted Stage 1 veins of the high quartz zone parallel main cleavage (S_1) with cross cutting Stage 3 related pyrite vein, 423150 E, 6265155 N. **c)** Open F_1 folded quartz veins in chlorite-quartz altered sandstone formed during the first phase of deformation, 423493 E, 6265539 N. **d)** Tight to isoclinal folded molybdenite-quartz veins and related pervasive cleavage formed in intense phyllic altered rocks during the first phase of deformation (F_1 , S_1), 423832 E, 6265290 N.

sulphide mineralogy in the breccia indicates: quartz, anhydrite, fluorite, calcite, gypsum, muscovite, illite, apatite, anatase, albite and chlorite together with pyrite, chalcopyrite, bornite, molybdenite, tennantite, enargite, sphalerite and traces of magnetite. The bornite breccia body preserves all four stages of mineralization with Stage 1 stockwork preceding breccia emplacement, and Stage 3 and Stage 4 veins and breccias cutting the body. Bornite and molybdenite disseminations in the same veins suggest that the bornite breccia is temporally associated with Stage 2 molybdenite mineralization. Anhydrite-fluorite-bornite-chalcopyrite assemblages in the bornite body also resemble the Stage 2 molybdenite veins peripheral to the core zone, which contain anhydrite and fluorite.

Stage 3 massive pyrite veins cut all phases of diorite, Stage 2 molybdenite veins, the high quartz zone (Fig. 15b) and the bornite breccia. Massive pyrite veins in the Mitchell zone are 1 mm to 3 cm wide and contain 60-95% medium- to coarse-pyrite grains. Gangue minerals are commonly quartz and muscovite that, together with disseminated pyrite, extend into

the country rock as a halo to the vein. Pyrite contains small inclusions of sphalerite, galena, chalcopyrite and tennantite. Margolis (1993) interpreted massive pyrite veins to be related to acid-sulphate style advanced-argillic alteration in the eastern Mitchell zone and the Snowfield gold zone. The late timing of our Stage 3 veins is consistent with this interpretation.

Stage 4 high-grade gold veins contain quartz, barite, calcite, and manganian calcite gangue minerals, with banded sulphides that include galena, sphalerite, tetrahedrite, electrum and tennantite. Stage 4 veins cut sandstone in the eastern part of the deposit, the bornite breccia and Stage 3 massive pyrite veins. Veins display sharp margins and euhedral to banded textures consistent with an epithermal origin. Minor bornite mineralization in Stage 4 veins that cut the bornite body is interpreted to have been remobilized during veining.

4.5. Mineralization

Most of the disseminated and vein-controlled copper and gold mineralization is related to Stage 1 alteration and Phase 1

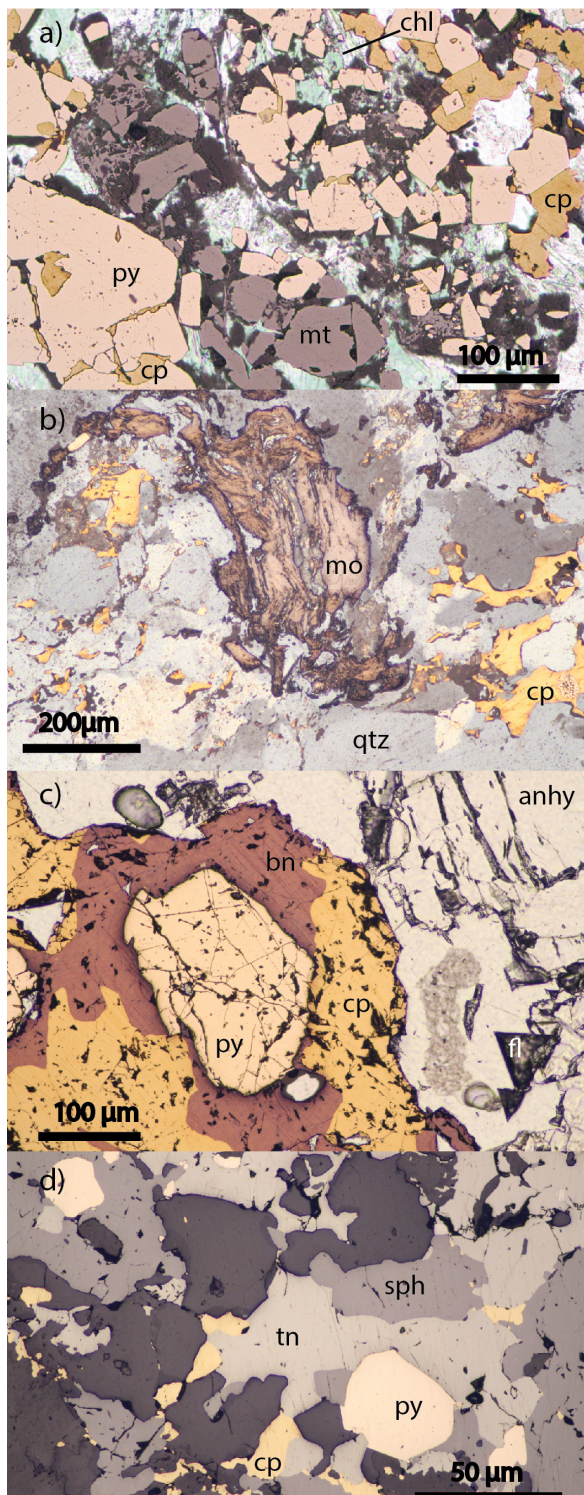


Fig. 16. Microtextures of chalcopyrite mineralization. **a)** Stage 1 cp: chalcopyrite with mt: magnetite and chl: chlorite replaces pyrite, reflected and plane polarized light, M-07-55, 255 m. **b)** Stage 2 mo: molybdenite and cp: chalcopyrite in quartz vein, reflected and cross polarized light M-08-70, 329 m. **c)** bn: bornite and cp: chalcopyrite replace py: pyrite and are spatially associated with anhy: anhydrite and fl: fluorite, reflected and plane polarized light, M-08-67, 251.3 m. **d)** Early py: pyrite is partially replaced by cp: chalcopyrite-sph: sphalerite-tn: tennantite in Stage 4 barite-quartz vein, reflected light, M-07-26, 212.6 m.

diorite plutonism. Chalcopyrite rims and replaces pyrite, occurs as inclusions in pyrite and as inclusions in and replacements of magnetite (Fig. 16a). Chalcopyrite and pyrite are inversely related; chalcopyrite to pyrite ratios generally decrease from the core outwards. Gold is microscopic and typically occurs as inclusions in sulphides or at sulphide grain boundaries. Copper and gold values are positively correlated and are notably homogeneous in their relative grade. Gold grades in general are proportional to the volume percent of quartz veins.

A molybdenum-rich shell envelopes the copper-gold core and is interpreted to have formed with Stage 2 phyllic alteration assemblages (Margolis, 1993) and Phase 2 diorite. The molybdenite to copper ratio increases from the core of the deposit outward. In the eastern, shallow levels of the system, molybdenite veins lack chalcopyrite. Although Stage 2 stockwork and mineralization are devoid of chalcopyrite at Snowfield (Margolis, 1993), we observed chalcopyrite and molybdenite-bearing veins in the transition zone between the core copper-gold and the molybdenite-rich shell at Mitchell (Fig. 16b).

Higher than average grades of copper and gold are intersected in the bornite breccia body and are interpreted to be the result of progressive upgrading during Stages 1 through 4 hydrothermal activity. Elevated copper grades correspond to high bornite to chalcopyrite ratios and are interpreted to have been introduced with anhydrite-fluorite-quartz (Fig. 16c).

High-grade Au-Ag-Pb-Zn-Cu mineralization associated with Stage 4 low sulphidation-type veins are superposed onto earlier (Stage 1-3) porphyry system stockwork and breccia bodies. Unlike porphyry-related mineralization, veins related to Stage 4 tend to have much higher tennantite to chalcopyrite ratios (Fig. 16d), higher gold and silver values, and visible sphalerite, galena and electrum grains. We consider that the veins are genetically related to porphyry emplacement and that their timing may correlate with porphyry-related epithermal mineralization at Brucejack (ca. 185 Ma; Pretium Resources, 2013). Epithermal veins cutting earlier stockwork zones suggest that uplift occurred between Stages 3 and 4. The Stage 4 veins lack significant mineralization in the drilled resource area but offer potential in the eastern Mitchell area.

4.6. Structure the Mitchell deposit

Three phases of progressive deformation related to mid-Cretaceous transpression and the formation of the Skeena fold and thrust belt, structurally modify the Mitchell deposit. The first phase is defined by a pervasive east-trending, near-vertical S_1 foliation, manifested by aligned chlorite and muscovite. Below the Mitchell thrust, the S_1 foliation (Fig. 17a) is subparallel to the sheeted Stage 1 quartz veins. Quartz veins are commonly folded into F_1 folds (Fig. 17b) that plunge steeply to the west, similar to the overall plunge of the orebody. West-northwest to west-southwest striking, steeply dipping predominantly sinistral strike slip faults (Fig. 8) are interpreted to have formed before and, possibly during the development of S_1 fabrics. S_1 foliation, in particular the limbs of F_1 folds, are

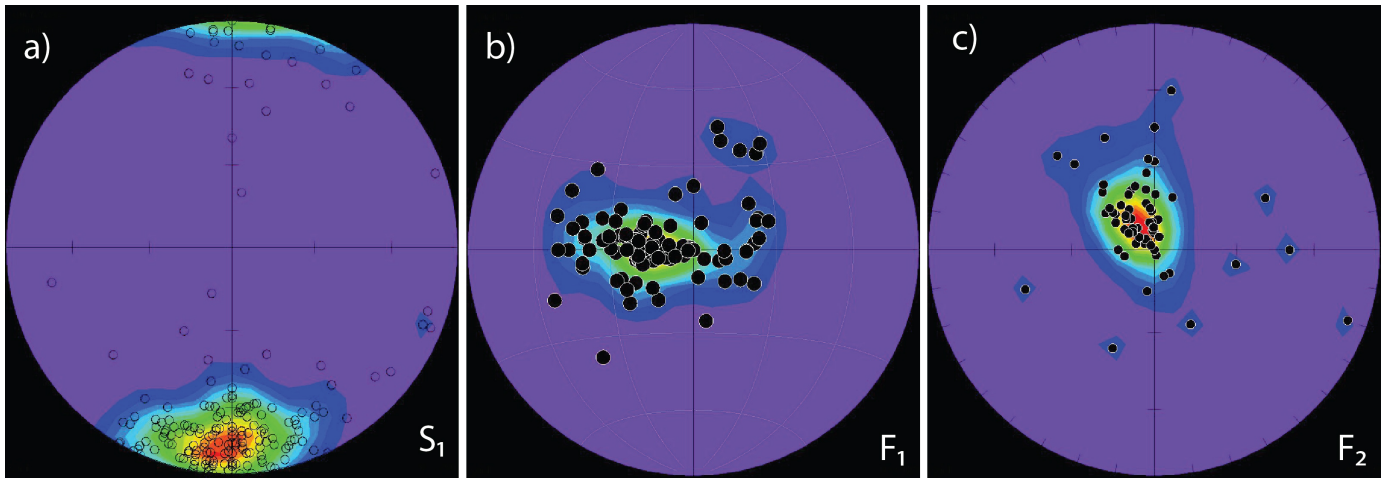


Fig. 17. a) Poles to S_1 cleavage. b) F_1 fold axes. c) F_2 fold axes.

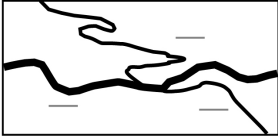
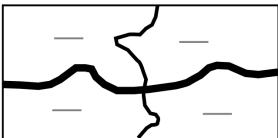
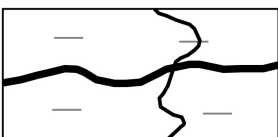
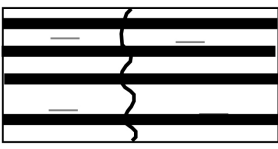
Alteration	Estimated flattening	Example	Folds
phyllic	50-70%		F_1 tight to isoclinal, F_2 gentle-open
intermediate argillic	20-50%		F_1 open-isoclinal, F_2 gentle-open
chlorite	20-40%		F_1 open, F_2 gentle
high quartz zone	10-30%		rare F_1 due to E-W vein geometry, gentle F_2
transitional potassic	5-10%		F_1 folds in thin veins
potassic and propylitic	0%		none

Fig. 18. Qualitative estimate of strain for altered rocks of the Mitchell zone as indicated by F_1 and F_2 fold morphology.

locally overprinted by steep north-northwest plunging, gentle-open F_2 folds (deformation phase 2; Fig. 17c).

Fold geometry is a function of alteration type (Fig. 18). Isoclinal F_1 folds in quartz veins are in intensely phyllic altered rocks; close folds are in, chlorite and intermediate argillic altered rocks, and folds are lacking in potassic altered rocks. Veins of the high quartz zone are sheeted and preferentially develop F_2 folds due to their east-west striking trends. Foliation is very well developed in the predominantly phyllic altered southeastern parts of the Mitchell zone and is poorly developed to non-existent in the western, potassic and transitional potassic areas (Fig. 14).

The Mitchell thrust fault (deformation phase 3; 110.2 ± 2.3 Ma; Ar-Ar illite; Margolis, 1993) is curvilinear, dips shallowly to the northwest and offsets the steeply plunging deposit ca. 1600 m to the southeast. The Mitchell thrust is in the footwall of the Sulphurets thrust and is interpreted as a younger, in-sequence foreland-propagating fault. The Mitchell thrust clearly truncates the east-west striking sheeted quartz veins and the subparallel east-west striking S_1 cleavage. The ore deposit is further imbricated by smaller thrust and reverse faults (Fig. 8) that are likely kinematically linked with the Mitchell thrust. Mineralization in the Mitchell deposit is offset at ca. 900 m depth by a 20 m thick deformation zone named here as the Mitchell Basal thrust observed in holes M-08-62 and M-08-67 (Figs. 7a, b).

5. Geochronology of the Mitchell deposit

Two Phase 1 and one Phase 2 medium-grained dioritic samples from the Sulphurets suite were collected for U-Pb zircon geochronology. One vein sample of molybdenite from the Mitchell deposit was collected from drill core for Re-Os geochronology.

5.1. Analytical methods: U-Pb zircon

Zircon analysis was by laser ablation-inductively coupled plasma-mass spectrometry (LA-ICP-MS) at the University of British Columbia's Pacific Centre for Isotopic and Geochemical Research; detailed methods are described by Tafti et al. (2009).

5.2. Analytical methods: Re-Os (molybdenite)

A molybdenite mineral separate was produced by metal-free crushing followed by gravity and magnetic concentration methods. Methods used for molybdenite analysis are described in detail by Selby & Creaser (2004) and Markey et al. (2007). The ^{187}Re and ^{187}Os concentrations in molybdenite were determined by isotope dilution mass spectrometry using Carius-tube, solvent extraction, anion chromatography and negative thermal ionization mass spectrometry techniques. A mixed double spike containing known amounts of isotopically enriched ^{185}Re , ^{190}Os , and ^{188}Os analysis is used. Isotopic analysis is made using a ThermoScientific Triton mass spectrometer by Faraday collector. Total procedural blanks for Re and Os are less than <3 picograms and 2 picograms, respectively, which are insignificant for the Re and Os concentrations in molybdenite.

The Chinese molybdenite powder HLP-5 (Markey et al., 1998), is analyzed as a standard. For this control sample over a period of two years, an average Re-Os date of 221.56 ± 0.40 Ma (1SD uncertainty, $n=10$) is obtained. This Re-Os age date is identical to that reported by Markey et al. (1998) of 221.0 ± 1.0 Ma. The age uncertainty is quoted at 2σ level, and includes all known analytical uncertainty, including uncertainty in the decay constant of ^{187}Re .

5.3. Results

5.3.1. Sample M-11-123; Phase 1 diorite

A medium-grained, potassic altered, Phase 1 diorite (sample M-11-123; Fig. 19a) sampled from a depth of 621 m yielded an age 196.0 ± 2.9 Ma (Fig. 19a). The intrusion is interpreted to be intramineral as it is host to Stage 1 related veins that are irregularly shaped, have diffuse boundaries, and are disarticulated. The sampled intrusion is diorite in composition from whole rock geochemistry (Fig. 13a). The porphyry contains 35% sericitized anorthitic plagioclase (0.5-2 mm in diameter), 7% K-feldspar (1-5 mm in diameter) with inclusions of hornblende in an altered, fine-grained groundmass (Fig. 20a). The sampled area is overprinted by pervasive and vein-controlled secondary K-feldspar, quartz, biotite, chlorite, magnetite, pyrite and chalcopyrite.

5.3.2. Sample GF-13-02; Phase 1 diorite

A medium-grained, chlorite and phyllic altered, Phase 1 diorite that outcrops adjacent to the high quartz zone (sample GF-13-02; 423312E, 6265278N; Fig. 8) yielded an age of 189 ± 2.8 Ma (Fig. 19b). The diorite is interpreted as a host rock to the high quartz zone in this location because there are no clasts of sheeted quartz veins in the intrusion and it appears to grade into the high quartz zone. The sampled intrusion is diorite in composition from whole rock geochemistry (Fig. 13a). The porphyry contains 35% sericitized laths interpreted to be replaced plagioclase (1-2 mm in diameter), 8% chlorite rhombohedral aggregates interpreted to be replaced hornblende (0.5-1 mm in diameter) and 5% equant anhedral K-feldspar partially replaced to sericite (2-3 mm diameter) in an altered, fine-grained groundmass (Fig. 20b). The intrusion is overprinted by Stage 2 sericite-chlorite-pyrite alteration with disseminations of secondary magnetite, trace chalcopyrite, 2% pyrite and ~10% quartz-chalcopyrite-pyrite veins by volume.

5.3.3. Sample M-07-49; Phase 2 diorite

A sample (M-07-49, 320 m; Fig. 7a) of fine-grained, Phase 2 diorite plug that cuts the high quartz zone and is overprinted by Stage 2 phyllic alteration yields an age of 192.2 ± 2.8 Ma (Fig. 19c). The high quartz zone that is cut by the plug contains 60-90% quartz-pyrite-chalcopyrite veins in the contact area. The sampled intrusion is diorite in composition from whole rock geochemistry (Fig. 13a) and contains 1-10% quartz vein xenoliths that are most abundant in the contact areas. The porphyry contains 30% sericitized laths (ca. 1 mm long) interpreted to be replaced plagioclase, 5% chlorite aggregates

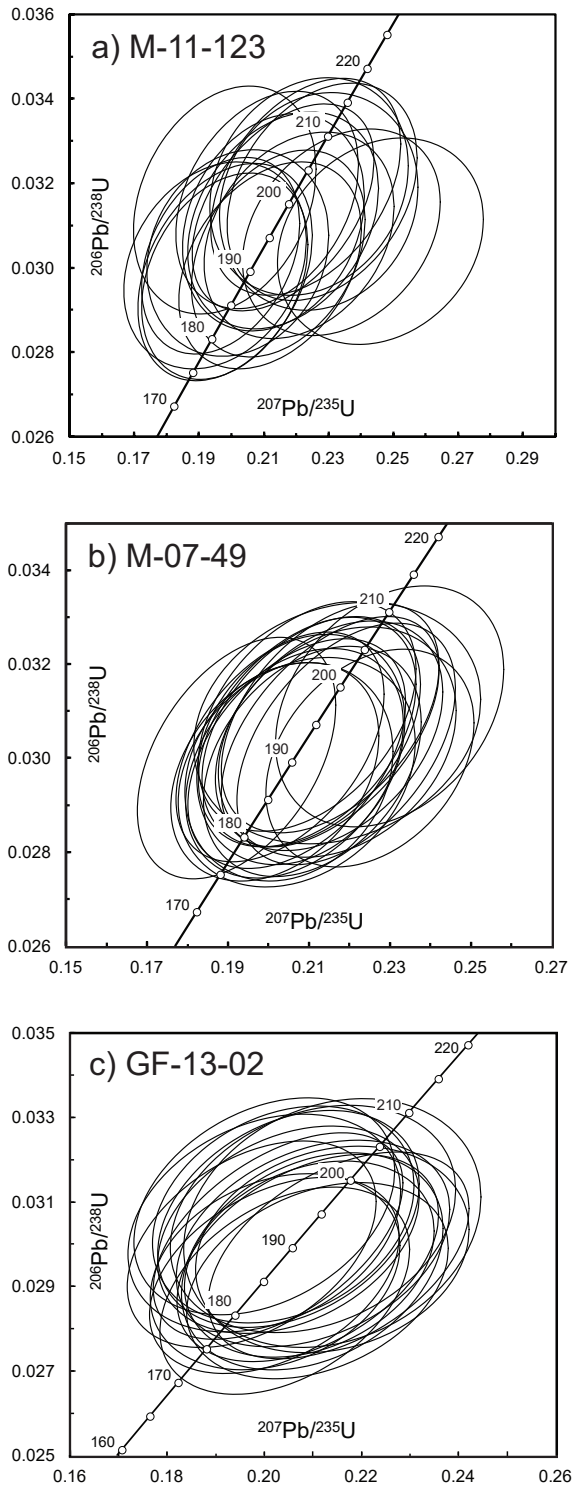


Fig. 19. U-Pb concordia diagrams for Sulphurets suite diorite in the Mitchell deposit. **a)** Sample M-11-123, **b)** sample M-07-49 and **c)** sample GF-13-02. See Figs. 7a, b, 8 for sample locations.

interpreted to be replaced hornblende, and 5% anhedral inclusion-rich K-feldspar in a fine-grained groundmass (Fig. 20c). The intrusion is overprinted by Stage 2 sericite-chlorite-pyrite alteration with 1% secondary magnetite, trace chalcopyrite and stringers of anhydrite and calcite.

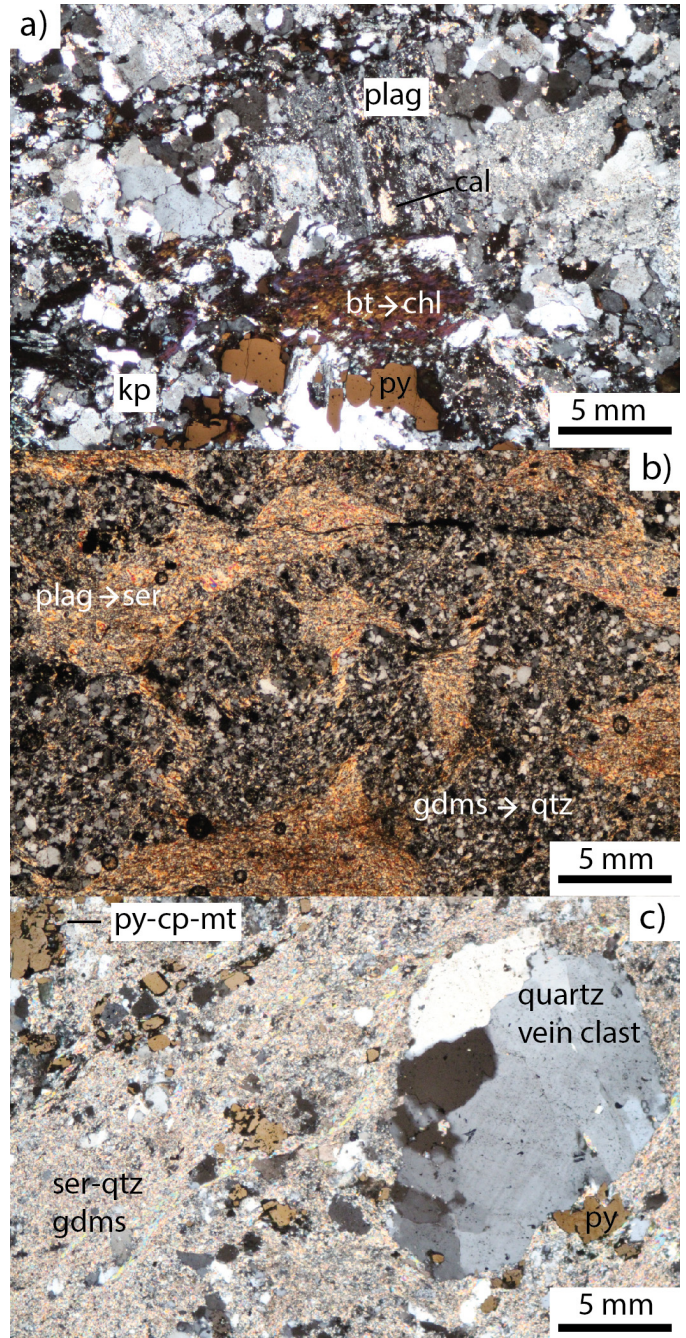


Fig. 20. Photomicrographs of the three dated Mitchell intrusions. **a)** Primary plag: plagioclase altered to cal: calcite, kp: K-feldspar replacement of groundmass and plagioclase, secondary bt: biotite replaced to chl: chlorite, sample M-11-123. **b)** Plagioclase ghosts are defined by sericite domains (plag->ser) and groundmass consists of quartz altered domains (gdms->qtz), sample GF-13-02. **c)** Phenocrysts and groundmass completely replaced by sericite-quartz (ser-qtz gdms), quartz vein clast (high quartz zone) and pyrite-chalcopyrite-magnetite (py-cp-mt) accompanies alteration, sample M-07-49.

5.3.4. Sample M-10-116, Stage 2 molybdenite vein (Re-Os)

Molybdenite in a sample (M-10-116, 214.6 m; Fig. 8) from a Stage 2 quartz-pyrite vein with yellow sericite alteration haloes in intensely sericite-pyrite-chlorite altered andesite breccia

yielded an Re-Os age of 190.3 ± 0.8 Ma. The vein host rock contains juvenile porphyritic angular andesite fragments ca. 60% clasts ca. 1 cm in diameter with <1% subrounded granule-sized felsic clasts. The host rock is intensely altered to sericite-pyrite-chlorite and is well foliated. The molybdenite-bearing vein is 3-4 mm wide with wavy margins, is parallel to foliation and contains a thin (1 mm) selvage of white and yellow sericite alteration. The vein contains 75% grey-white microcrystalline quartz, 15% blue-grey elongate molybdenite disseminations, 8% brass-yellow anhedral to subhedral pyrite disseminations (<0.2 mm) and 2% sericite.

5.3.5. Geochronologic summary

Phase 1 plutonism and Stage 1 alteration and copper-gold mineralization are bracketed between 196.0 ± 2.9 Ma and 189.9 ± 2.8 Ma. The crystallization age of Phase 2 rocks is 192.2 ± 2.8 Ma, close to the age of molybdenite mineralization (190.3 ± 0.8 Ma), which we consider records Stage 2 alteration and mineralization. Advanced argillic, Stage 3 and Phase 3 plutonism are interpreted to be younger than 190.3 ± 0.8 Ma.

6. Discussion

6.1. Evolution of the Mitchell deposit

The most significant mineralization and alteration event (Stage 1) was coeval with Phase 1 Sulphurets diorite intrusion, potassic and propylitic alteration, and the formation of a copper-gold core zone (Fig. 21a; Table 2). An east-striking, steeply dipping sheeted high quartz zone (>60% volume of quartz) is developed in the contact area between Phase 1 diorite and Stuhini Group rocks or overlying Jack Formation (Fig. 21a). A Stage 2 molybdenite shell envelopes a Phase 2 Sulphurets diorite plug in the core region of the deposit related to overprinting phyllic and intermediate argillic alteration. The alteration developed laterally in Jack Formation sandstone and penetrated along fractured stockwork zones at deeper levels (Fig. 21b; Table 2). The molybdenite shell is contiguous with the core zone copper-gold stockwork emplaced during Stage 1 and Stage 2 events. Poorly mineralized massive Stage 3 pyrite veins are temporally related to a small Phase 3 Sulphurets diorite plug advanced argillic alteration in the southeastern Mitchell zone, and widespread advanced argillic alteration in the Snowfield zone (Fig. 21c; Table 2). Stage 3 alteration lacks

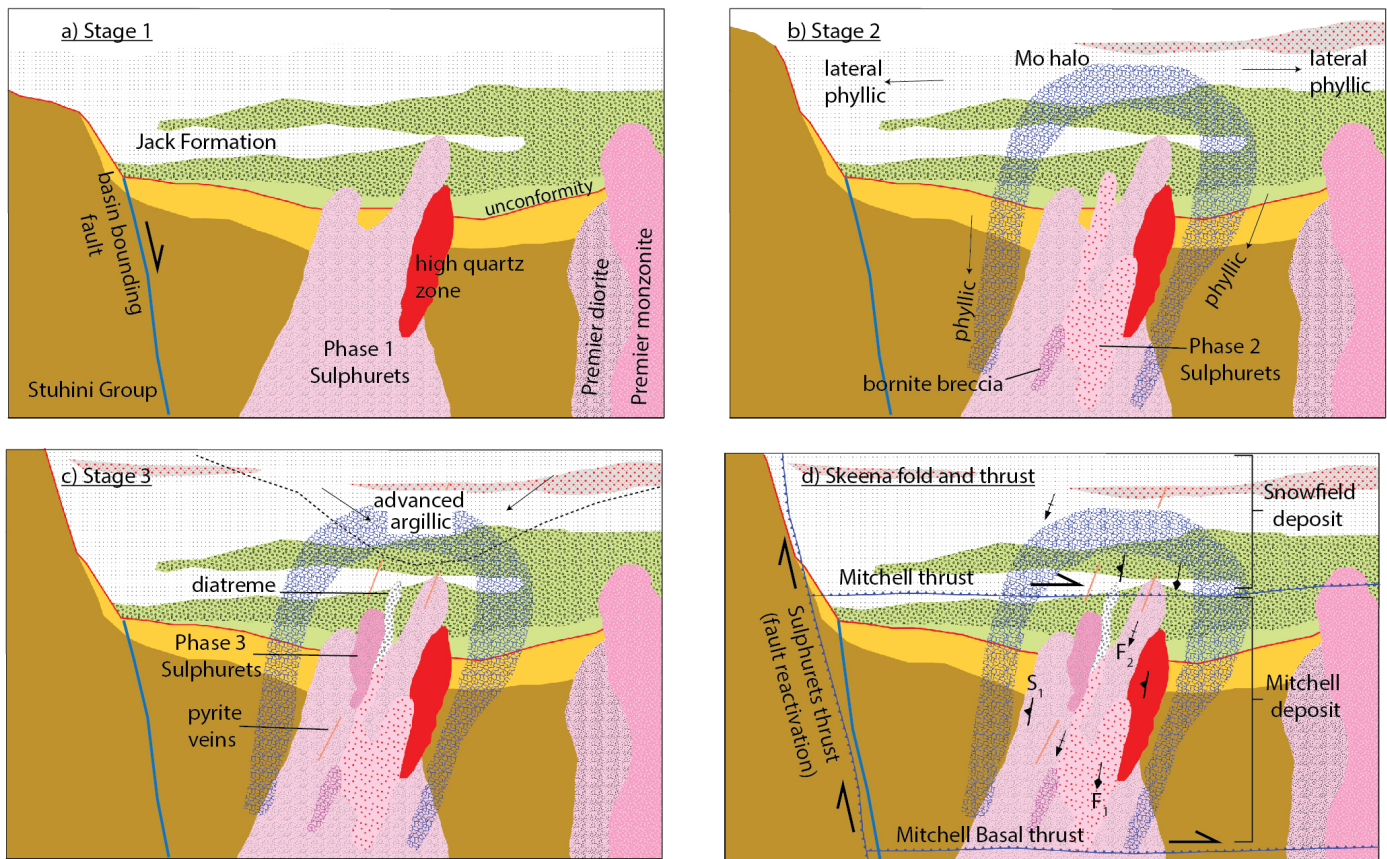


Fig. 21. Model for the evolution of the Mitchell deposit. **a)** Stage 1 alteration and mineralization is related to emplacement of Phase 1 diorite and the high quartz zone after Premier diorite and monzonite intrusion; **b)** Stage 2 phyllic alteration is related to a molybdenite-rich envelope, Phase 2 diorite and the bornite breccia; **c)** Stage 3 advanced argillic alteration at shallow levels is related to massive pyrite veins, Phase 3 diorite and the diatreme breccia; **d)** Mid-Cretaceous deformation related to Skeena fold and thrust belt; S_1 pervasive cleavage F_1 , F_2 folds and D_3 Mitchell thrust, Mitchell Basal thrust and the Sulphurets thrust.

significant mineralization. Epithermal textures in Stage 4 veins suggest uplift during a hiatus of hydrothermal activity between Stages 3 and 4.

In the mid-Cretaceous, three phases of progressive deformation modified the deposit. Pervasive east-west striking S_1 cleavage and associated steeply west-plunging F_1 folds are overprinted by steeply north-plunging F_2 fold trends similar to the McTagg Anticlinorium, and the Mitchell thrust fault separated the Snowfield and Mitchell zones (Fig. 21d).

6.2. The Mitchell deposit: a calc-alkalic porphyry

The shallower porphyry deposits of the Sulphurets district have been variously classified as alkalic and calc-alkalic. For example, Logan and Mihalynuk (2014) referred to the Kerr deposit as calc-alkalic Bissig and Cooke (2014) designated the KSM deposits as a whole as silica-saturated alkalic. At Sulphurets, quartz veins and molybdenum content are considered characteristic of calc-alkaline magmatism whereas the composition of the intrusions and alteration types are more typical of alkalic systems (Fowler and Wells, 1995). Ditson et al. (1995) suggested the core chlorite with phyllic alteration halo at Kerr is atypical of British Columbia porphyry deposits and does not fit either alkalic or calc-alkalic models. Margolis (1993) interpreted early Cu-Au mineralization at Snowfield as a result of alkaline magmatism and related molybdenum and sericitic alteration (uncommon to alkaline systems) to a younger overprint. Pretium Resources (2013) considers epithermal high grade gold veins at Brucejack to be genetically related to alkaline Cu-Au porphyry mineralization at KSM.

Although the Mitchell deposit shares characteristics with alkalic porphyry systems, such as relatively high gold grades and magnetite in alteration assemblages (Bissig and Cooke,

2014), we consider the Mitchell a calc-alkalic porphyry deposit because: 1) the Sulphurets suite is subalkaline; 2) phyllic and clay alteration assemblages are abundant, 3) alteration assemblages contain high pyrite concentrations throughout; 4) alteration is extensive (>4 km wide; Fig. 14); 5) silica contents in the ore zone are high (5-95% volume quartz veins); 6) it contains economically significant molybdenum mineralization; and 7) of the scale of the deposit (>4.5 billion tonnes of inferred resources combining the Mitchell and Snowfield; Pretium Resources, 2011; Seabridge Gold, 2014).

6.3. The relationship between the Snowfield and Mitchell deposits

The Snowfield deposit occupies the hanging wall of the Mitchell thrust fault ca. 1.6 km east-southeast of the Mitchell deposit and is interpreted to be the shallower continuation of the Mitchell deposit (Fig. 21). We base this interpretation on the following: 1) metal zonation patterns indicate a core zone of elevated copper and gold with a shell of molybdenum-rich ore common to both deposits separated by the Mitchell thrust (Fig. 22; Savell and Threlkeld, 2013); 2) the Snowfield mineralization is hosted in Mitchell intrusions and Jack Formation quartz-bearing sandstone and conglomerate in the highest stratigraphic levels of the Mitchell zone; 3) the Snowfield deposit is composed predominantly of phyllic and argillic alteration assemblages whereas in the Mitchell deposit phyllic alteration is limited to shallow and easterly regions and penetrations at depth suggesting continuity of alteration assemblages between the two deposits. Margolis (1993) considered the advanced argillic alteration intensity in the Snowfield stockwork as evidence that it is a shallower system than the Mitchell stockwork. The Mitchell-Snowfield system

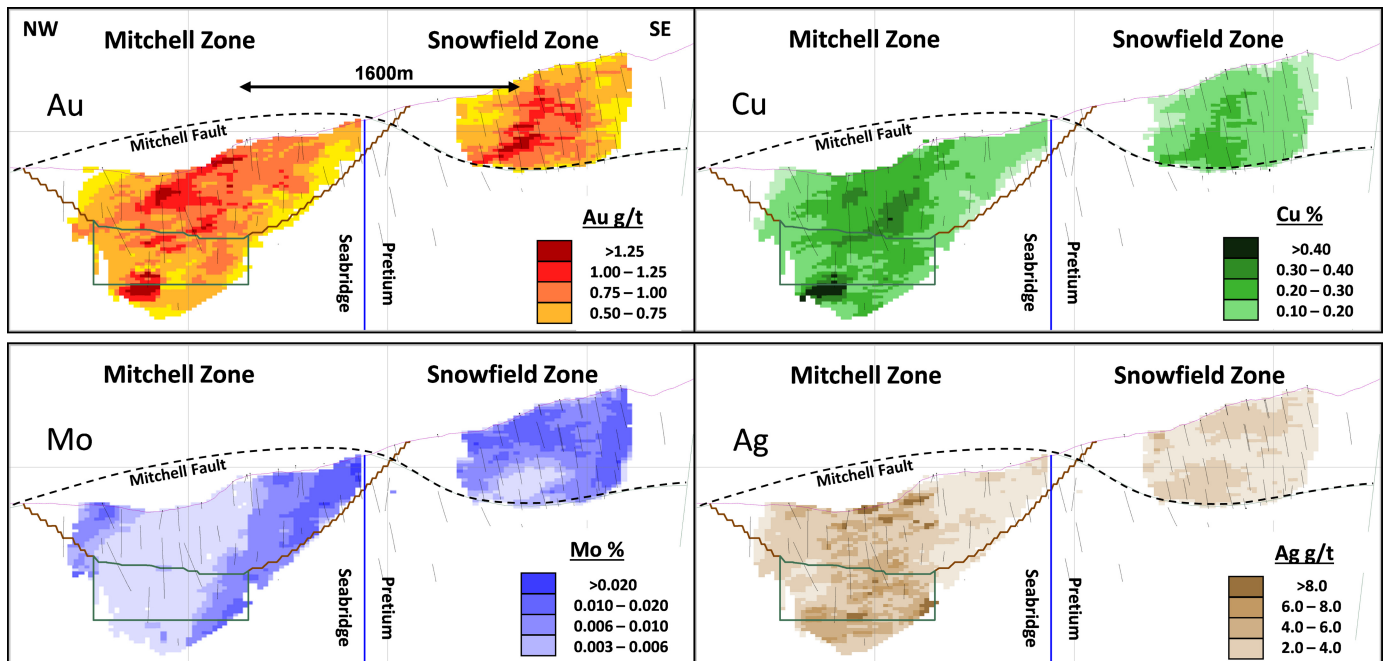


Fig. 22. Au, Cu, Ag and Mo metal grades of the Mitchell and Snowfield deposit, after Savell and Threlkeld (2013).

is interpreted as a north-plunging, fault-dissected ore body that grades from Jack Formation sandstone hosted stockwork on surface in the Snowfield deposit to intrusion-hosted stockwork at depth in the Mitchell deposit.

7. Conclusion

The calc-alkalic Mitchell deposit formed during emplacement of Sulphurets suite dioritic magmatism and is interpreted to be the deeper levels of a once contiguous, gigantic porphyry deposit that included the structurally offset Snowfield deposit. The Mitchell-Snowfield mineral system was likely active for at least 2 million years. Mineralization is related to Sulphurets suite plagioclase-hornblende intrusions that cut and overprint earlier Premier suite monzonite and syenite intrusions. Three new U-Pb zircon ages for the Sulphurets suite diorite and a Re-Os molybdenite age indicate that magmatic-hydrothermal mineralizing processes started after 196.0 ± 2.9 Ma and ended before 189.9 ± 2.8 Ma.

Acknowledgments

This research was made possible by a generous financial contribution from Seabridge Gold Inc to LAK in addition to in-kind support throughout the project. We are grateful to the Seabridge Gold management team especially: Rudi Fronk, Bill Threlkeld, Tim Dodd, Peter Erwich, James Freeman and Tom Kraft for the tremendous support and involvement in the research project. GEF is grateful to Pretium Resources Inc, namely Ken McNaughton, Charlie Grieg and Warwick Board, for permission to map parts of the Mitchell and Snowfield deposits and for valuable input throughout the project. Many thanks to Paul Wojdak and JoAnne Nelson for discussions about the Mitchell zone, which have contributed much to our understanding of the deposit. This manuscript was greatly improved by detailed and thoughtful reviews by Lawrence Aspler, JoAnne Nelson, and Jim Logan.

References cited

- Alldrick, D.J., 1993. Geology and metallogeny of the Stewart mining camp, northwestern British Columbia, British Columbia Ministry of Energy, Mines and Petroleum Resources, British Columbia Geological Survey Bulletin 85, 105 p.
- Alldrick, D.J., and Britton, J.M., 1988. Geology and mineral deposits of the Sulphurets area. British Columbia Ministry of Energy, Mines and Petroleum Resources, British Columbia Geological Survey Bulletin 85, 105 p.
- Alldrick, D.J., and Britton, J.M., 1991. Sulphurets area geology. British Columbia Ministry of Energy, Mines and Petroleum Resources, British Columbia Geological Survey Open File 1991-21, 1:20,000 scale.
- Anderson, R.G., 1989. A stratigraphic, plutonic, and structural framework for the Iskut River map area, northwestern British Columbia; in Current Research, Part E, Geological Survey of Canada, Paper 89-1E, pp. 145-154.
- Bissig, T., and Cooke, D.R., 2014. Introduction to the Special Issue devoted to alkalic porphyry Cu-Au and epithermal Au deposits: Economic Geology, Special Issue on Alkalic Porphyry Deposits, 109, pp. 819-825.
- Bridge, D.J., 1993. The deformed Early Jurassic Kerr copper-gold porphyry deposit, Sulphurets gold camp, northwestern British Columbia, unpublished M.Sc. thesis, University of British Columbia.
- Disson, G.M., Wells, R.C., and Bridge, D.J., 1995. Kerr: The geology and evolution of a deformed porphyry copper-gold deposit, northwestern British Columbia. In: Porphyry Deposits of the Northwestern Cordillera of North America, T.G. Schroeter, (Ed.), Canadian Institute of Mining, Metallurgy and Petroleum, Special Volume 46, pp. 509-523.
- Evenchick, C.A., 2001. Northeast-trending folds in the western Skeena Fold Belt, northern Canadian Cordillera: a record of Early Cretaceous sinistral plate convergence: Journal of Structural Geology, 23, 1123-1140.
- Evanchick, C.A., McMechan, M.E., McNicoll, V.J., and Carr, S.D., 2007. A synthesis of the Jurassic-Cretaceous tectonic evolution of the central and southeastern Canadian Cordillera: exploring the links across the orogeny. In: Sears, J.W., Harms, T.A., and Evanchick, C.A., (Eds.), Whence the mountains? Inquiries into the evolution of orogenic systems. A volume in honour of Raymond A. Price. Geological Society of America, Special Paper 433, pp. 117-145.
- Fowler, B.P., and Wells, R.C., 1995. The Sulphurets Gold zone, northwestern British Columbia, Porphyry Deposits of the Northwestern Cordillera of North America, Schroeter, T.G., (Ed.), Canadian Institute of Mining, Metallurgy and Petroleum, Special Volume 46, pp. 484-498.
- Greig, C.J., 1992. Fieldwork in the Oweege and Snowslide ranges and Kinskuch Lake area, Northwestern BC. In: Current Research, Part A. Geological Survey Paper 92-1A, pp. 145-155.
- Hansley, P., 2008. Petrography of samples from the Kerr-Sulphurets-Mitchell property, Petrographic Consultants International Inc., unpublished report prepared for Seabridge Gold Inc.
- Hastie, A.R., Kerr, A.C., Pearce, J.A., and Mitchell, S.F., 2007. Classification of altered volcanic island arc rocks using immobile trace elements: development of the Th-Co discrimination diagram. Journal of Petrology, 48, 2341-2357.
- Henderson, J.R., Kirkham, R.V., Henderson, M.N., Payne, J.G., Wright, T.O., and Wright, R.L., 1992. Stratigraphy and structure of the Kerr-Sulphurets area, British Columbia, Current Research, Part A, Geological Survey of Canada, Paper 92-1A, pp. 323-335.
- Kirkham, R.V., 1963. The geology and mineral deposits in the vicinity of the Mitchell and Sulphurets glaciers, Northwest British Columbia, unpublished M.Sc.thesis, University of British Columbia, 142 p.
- Kirkham, R.V., and Margolis, J., 1995. Overview of the Sulphurets area, northwestern British Columbia, Porphyry Deposits of the Northwestern Cordillera of North America, Schroeter, T.G., (Ed.), Canadian Institute of Mining, Metallurgy and Petroleum, Special Volume 46, pp. 473-483.
- Kramer, R., 2014. Structural geology of the Kerr Deposit Iskut-Stikine region, British Columbia, unpublished B.Sc. thesis, University of British Columbia.
- Lewis, P.D., 1992. Structural Evolution of the Iskut River Area: Preliminary results. Mineral Deposit Research Unit, The University of British Columbia Annual Technical Report-Year 2, pp. 2.1-2.21.
- Lewis, P.D., 2001. Geological maps of the Iskut River area. In: Lewis, P.D., Toma, A., and Tosdal, R.M., (Eds.), Metallogensis of the Iskut River area, northwestern British Columbia. Mineral Deposit Research Unit, Special Publication Number 1, 77-83.
- Lewis, P.D., Mortensen, J.K., Childe, F., Friedman, R., Gabites, J., Ghosh, D., and Bevier, M.L., 2001. Geochronology data set in the Iskut River area-progress and problems: metallogensis of the Iskut River area, northwestern British Columbia, Mineral Deposit Research Unit, Special Publication Number 1, pp. 89-96.
- Lewis, P.D., 2013. Iskut River area geology, northwest British Columbia. Geoscience British Columbia Report 2013 -05, 3

- 1:50,000 scale maps, legend and notes.
- Logan, J.M., Drobe, J.R., and McClelland, W.C., 2000. Geology of the Forrest Kerr-Mess Creek area, northwest British Columbia (NTS 104B/10, 15 & 104/G2 & 7W). British Columbia Ministry of Energy, Mines and Petroleum Resources, British Columbia Geological Survey Bulletin 104, 163 p.
- Logan, J.M., and Mihalynuk, M.G., 2014. Tectonic controls on early Mesozoic paired alkaline porphyry deposit belts (Cu-Au+Ag-Pt-Pd-Mo) within the Canadian Cordillera: Economic Geology, Special Issue on Alkalic Porphyry Deposits, 109, 827-858.
- Markey, R., Stein, H.J., Hannah, J.L., Zimmerman, A., Selby, D., and Creaser, R.A., 2007. Standardizing Re-Os geochronology: a new molybdenite reference material (Henderson, USA) and stoichiometry of Os salts. *Chemical Geology*, 244, 74-87.
- Markey, R., Stein, H., and Morgan, J., 1998. Highly precise Re-Os dating for molybdenite using fusion and NTIMS. *Talanta*, 45, 935-946.
- Margolis, J., 1993. Geology and intrusion-related copper-gold mineralization, Sulphurets, British Columbia, unpublished Ph.D. thesis, University of Oregon, 289 p.
- Nelson, J., and Kyba, J., 2014. Structural and stratigraphic control of porphyry and related mineralization in the Treaty Glacier-KSM-Brucejack-Stewart trend of western Stikinia. In: *Geological Fieldwork 2013*, British Columbia Ministry of Energy and Mines, British Columbia Geological Survey Paper 2014-1, pp. 111-140.
- Pretium Resources, 2011. Snowfield project website: <http://www.pretium.com>. Snowfield mineral resource summary, February, 2011.
- Pretium Resources, 2013. Brucejack project website: <http://www.pretium.com>. Report on Brucejack property geology, April, 2013.
- Pretium Resources, 2014. Brucejack project website: <http://www.pretium.com>. Brucejack project reserves and resources summary, June, 2014.
- Savell, M., and Threlkeld, B., 2013. The KSM project-a cluster of porphyry related, deformed and dismembered Au-Cu-Mo deposits displaying a transition from deep porphyry to shallow vein environments, Seabridge Gold Inc. website: http://seabridgegold.net/pdf/geology/KSM_Geology_update_Sep_2013.pdf.
- Seabridge Gold, 2014. Reserves and resources website: <http://seabridgegold.net>. Mineral reserves and resources, March 11, 2014.
- Selby, D., and Creaser, R.A., 2004. Macroscale NTIMS and microscale LA-MC-ICP-MS Re-Os isotopic analysis of molybdenite: testing spatial restrictions for reliable Re-Os age determinations, and implications for the decoupling of Re and Os within molybdenite. *Geochimica et Cosmochimica Acta*, 68, 3897-3908.
- Simpson, T.M., 1983. The geology and hydrothermal alteration of the Sulphurets deposits, Northwest British Columbia, unpublished M.Sc. thesis, University of British Columbia, 99 p.
- Tafti, R., and Mortensen, J.K., 2009. Jurassic U-Pb and Re-Os ages for the newly discovered Xietongmen Cu-Au porphyry district, Tibet, PRC: implications for metallogenic epochs in the southern gangdese belt. *Economic Geology*, 104, 127-136.
- Visual Capitalist, 2013. Global gold mine and deposit rankings 2013 website: <http://www.visualcapitalist.com/wp-content/uploads/2013/11/global-gold-mine-and-deposit-rankings-2013.pdf>.
- Winchester, J.A., and Floyd, P.A., 1977. Geochemical discrimination of different magma series and their differentiation products using immobile elements. *Chemical Geology*, 20, 325-343.